UNIVERSITAT POLITÈCNICA
DE CATALUNYA
BARCELONATECH

Programa de Doctorat en Enginyeria Biomèdica
Departament d'Enginyeria de Sistemes,
Automàtica i Informàtica Industrial
Centre de Recerca en Enginyeria Biomèdica

Tesis Doctoral por compendio de publicaciones

Muscular pattern based on multichannel surface EMG during voluntary contractions of the upper-limb

Mislav Jordanić

Setembre 2017

Directores:
Miguel Angel Mañanas Villanueva
Mónica Rojas-Martínez

Abstract

Extraction of neuromuscular information is an important and extensively researched issue in biomedical engineering. Information on muscle control can be used in numerous human-machine interfaces and control applications, including rehabilitation engineering, e.g., prosthetics, exoskeletons and rehabilitation robots.

Neuromuscular information can be extracted at the brain level, peripheral nerves, or muscles. Among these options, muscle interface is the only viable way of information extraction in everyday life. Although brain and nerve recordings are promising, they usually require invasive measurement and achieve relatively low extraction speed which prevents real time control. Even though in electromyographic (EMG) recordings information is not obtained directly from neural cells, it contains similar information as nerve recording. Information contained in action potential of the innervated muscle fibers (MUAP) is equivalent to the information contained in the action potential of corresponding motor neurons. Moreover, muscles contain multiple motor units that activate simultaneously so their electrical activity sums on the surface of the skin, resulting in a relatively high amplitude compared to the other bioelectrical signals. Therefore, due to the richness of neural information, noninvasiveness and high signal-to-noise ratio, the surface EMG is extensively used for man–machine interfacing, especially in commercial/clinical upper-limb prosthetic control.

Motivation and merit of this thesis lies in the fact that information associated with muscular pattern during exercises can be very useful in different applications such as monitoring patients' control strategies during recovery, personalizing rehabilitation processes to increase their effectiveness or to provide information to be used for control of external devices (EMG based control of prosthesis or exoskeletons).

Within this doctorate a pattern recognition approach was used to assess neuromuscular information and to identify subjects' intended motion based on multichannel surface electromyographic recordings. Research was focused on control strategies of upper-limb, both in normal subjects and in patients with impaired mobility caused by incomplete spinal cord injury. Methods which are proposed can be used for the design and monitoring of rehabilitation therapies intended for patients with neuromuscular impairment, as well for the control of external devices like rehabilitation robots, exoskeletons, prostheses and even virtual games. However, that is in the domain of future applications and is not the scope of the thesis.

Contents

List of Tables

List of Figures

Chapter 1

Introduction

Performing a movement is a complicated process that involves many physiological entities working in high coherence. It involves bones, tendons, nerves, and many other working in perfect harmony. Even the simplest movements are rarely performed using just one muscle. Everything we do involves high muscular coordination and constant and precise regulation. While standing, muscles of legs and trunk are constantly simultaneously co-contracting, maintaining balance. Muscle is a body tissue capable of transforming chemical energy to force. There are several muscle types: smooth, building internal organs, cardiac, building the heart, and skeletal. Only skeletal muscles can be controlled voluntarily and are used in locomotion. They are usually connected to bones with tendons (collagen fibers), as shown in figure 1.3.

The neurons controlling the movement are organized in hierarchical fashion (Widmaier et al., 2003). In the highest level of hierarchy, the movement is conceived. Here the complex plan of intention is made. Very little is known about the exact location of neurons responsible for this task. Higher centers then transmit this command to the middle level structures, where the task is elaborated. Simultaneously, this middle level neurons receive the information from the receptors in muscles, skin, tendons, and join, but also from the visual system. Planning of the movement that is about to be performed is performed with respect to the space this movement will occupy, and detailed control signals for each muscle involved in the movement are generated. Centers involved in this tasks are located in cerebral cortex, cerebellum, subcortical nuclei, and brainstem. The information is then transmitted to the lowest level of the motor hierarchy:

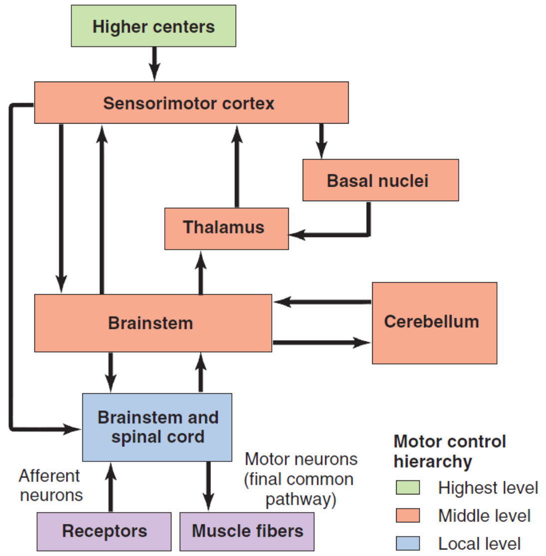

(a)

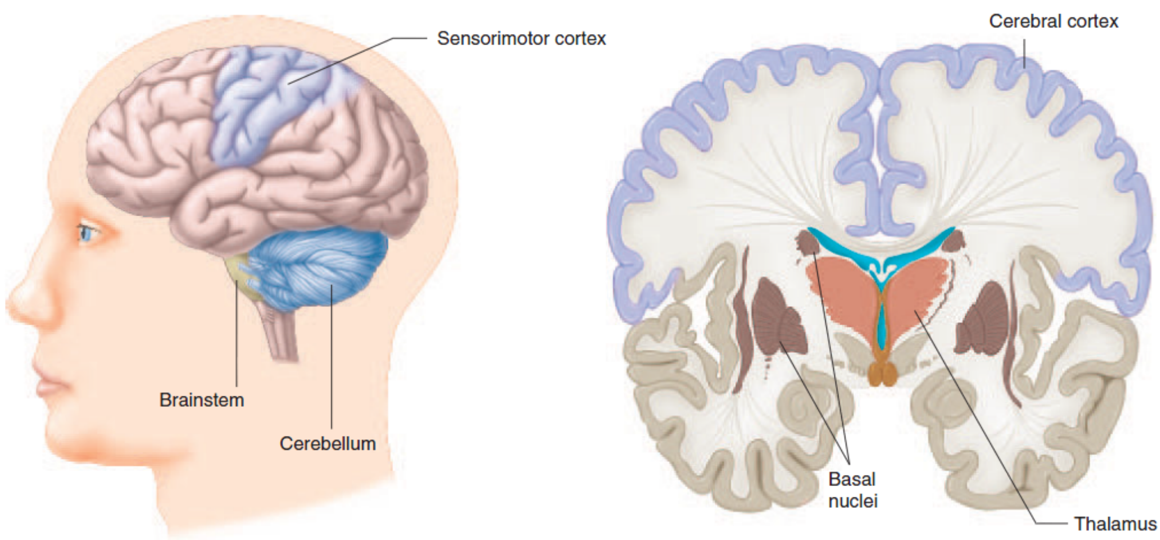

(b)

Figure 1.1: Figure describes **a)** hierarchical organization of neural system for motor control and **b)** side view and cross section of the brain showing motor control centers. Retrieved from (Widmaier et al., 2003)

spinal cord and brainstem. Here the information is transmitted over motor neurons to the muscles. The selection of motor neurons involved in the task and timing is performed at this level. Organization and locations of the neural system for motor control can be seen in figure 1.1, whereas overall figure of motor control can be seen in figure 1.2.

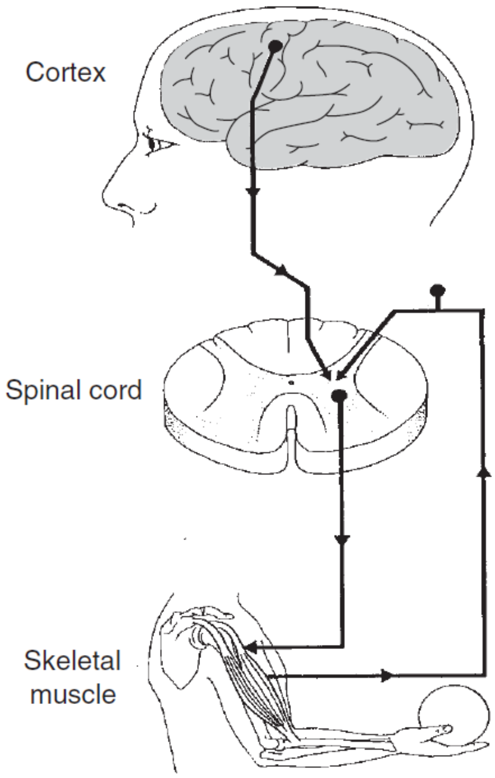

Figure 1.2: Figure represents a schematic representation of motor control mechanisms. Idea of a movement is conceived in the brain, and is getting to spinal cord by neural pathways. Motor neurons exiting spinal cord trigger muscle contraction. Simultaneously, sensory information is being transmitted to the higher controlling mechanisms. Retrieved from (Merletti and Parker, 2004)

1.1 Muscle physiology

Elementary building block of a muscle is muscle cell, or muscle fiber - *myocyte*. They are ensheated by *endomysium*, a connective tissue that contains nerves and capillaries. Myocytes are organized in bundles of 10 to 100 fibers, which are called *fascicles*, and they are surrounded by sheath of connective tissue, *perymisium*. Group of fascicles is finally grouped together and enveloped by *epimysium*, forming a muscle. Muscle can be seen in figure 1.3.

Sarcolema is the cell membrane of myocyte, consisting of a lipid bilayer that contains intracelular liquid, *myoplasma*. In the myoplasma, thin and thick filaments are serially connected, forming *sarcomeres*, which are longitudinally connected in *myofibrils* that extend through entire length of the myocyte. During shortening of muscle fibers, thin and thick filaments of sarcomeres are pulled together by cross-bridges between them. Total shortening of myofibril is summation of

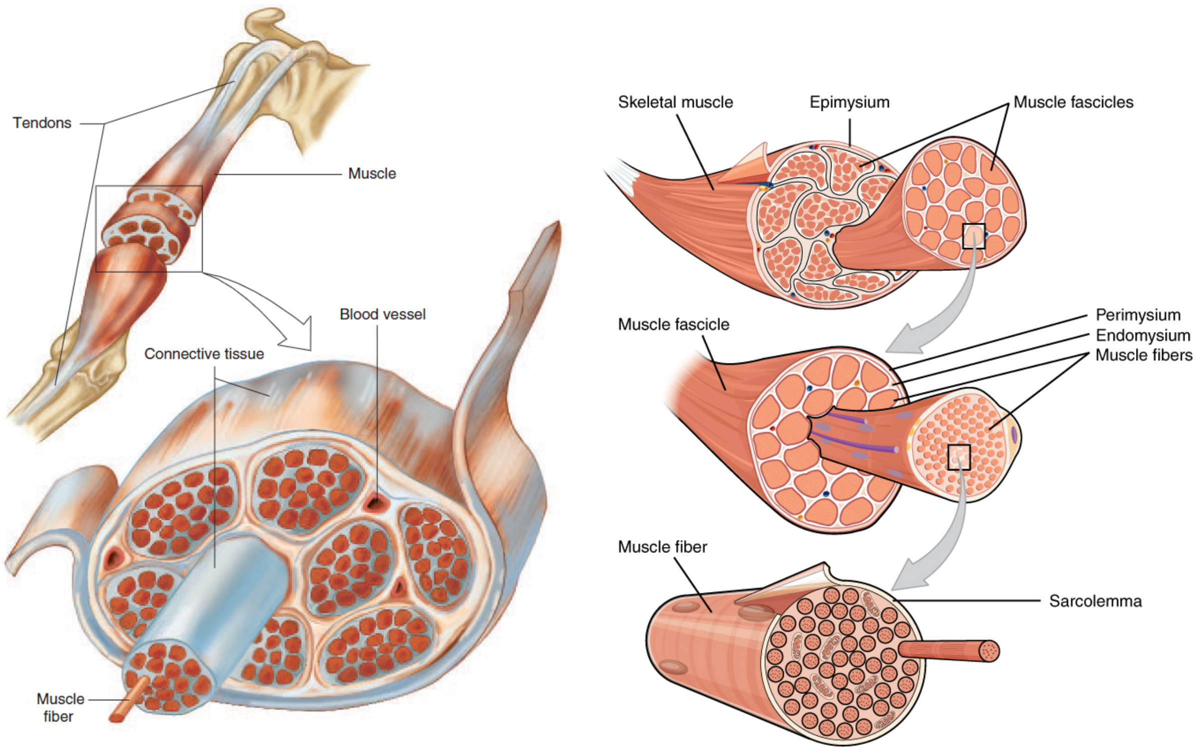

(a) Retrieved from Widmaier et al. (2003) (b) Retrieved from OpenStax (2013)

Figure 1.3: Figure shows **a)** cross-section of a skeletal muscle with attachment to a bone, and **a)** a detailed cross-section of skeletal muscle from myofibrils to entire muscle.

shortenings of sarcomeres of which it is composed.

Each motor neuron at the neuromuscular junction innervates several muscle fibers, forming the smallest functional unit called *motor unit*. It was firstly defined by Liddell and Sherrington in 1925 (Liddell and Sherrington, 1925; Sherrington, 1925) and is composed of motor neuron with axon and dendrites, and muscle fibers that axon innervates, as seen in the figure 1.4 (Duchateau and Enoka, 2011). Since motor neuron with a single action potential usually evokes action potentials simultaneously in all belonging muscle fibers, by observing action potentials of the muscle fibers, information on activity of motor neurons in spinal cord or brain stem can be inferred (Merletti and Farina, 2016). Pool of motor neurons that innervates entire muscle generally ranges from ten to thousand, depending on the muscle (Merletti and Farina, 2016).

By the characteristics of muscle fiber, there are three main types of muscle fibers:

Fast twitch, fatigable fibers (FF, or type IIb): This fiber type have high levels of ATP (source of energy) for anaerobic energy supply, and are dominantly present in pale muscles.

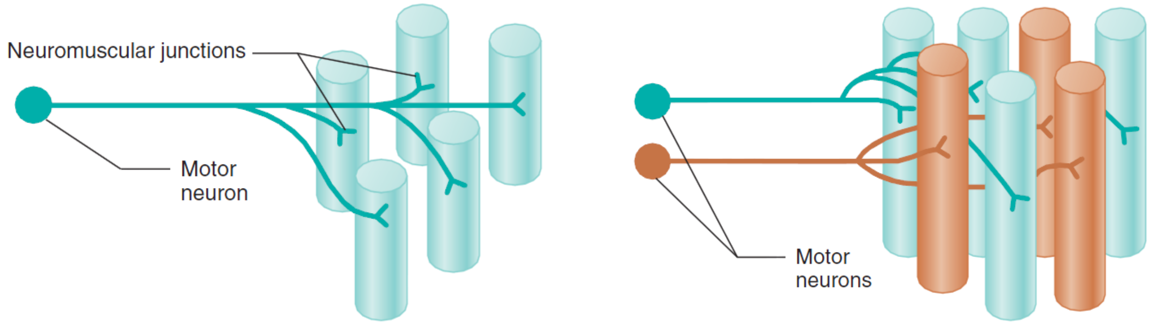

(a) (b)

Figure 1.4: Figure shows **a)** a single motor unit with motoneuron and muscle fibers it innervates, and **b)** two motor units where it can be seen how muscle fibers of different motor units are intermingled. Retrieved from (Widmaier et al., 2003)

They are of glycolytic type and work well in ischemic or low oxygen conditions. Regarding contraction properties, they are characterized by fast twitch, large forces and high nerve conduction velocity, but they get fatigued faster than the other muscle fiber types.

Fast twitch, fatigue-resistant (FR, or type IIa): These are oxidative glycolytic fibers, characterized by fast twitch and are resistant to fatigue. They have intermediate conduction velocity.

Slow twitch, very resistant to fatigue (S, or type I): They are slow oxidative fibers and do not work well in low oxygen conditions. They generate small forces, have slow twitch and are characterized by lower nerve conduction velocity. This fiber type is very resilient to fatigue because of high oxidative metabolism and energy efficiency. They are present in high percentage in red muscles, such as soleus.

Muscle fibers innervated by the same motor neuron have similar histochemical and contractile characteristics, and can be said that motor unit is composed of the muscle fibers of the same type.

Force that muscle fibers generate depends on firing frequency of the action potentials (rate coding) innervating the neuromuscular junction, and the recruitment strategy by which the motor units are activated, i.e., the number of activated motor units. Firing frequency and the recruitment strategy depend on the speed and force of contraction. Muscle units with low threshold are activated firstly, resulting in low force and high endurance, i.e., resistance

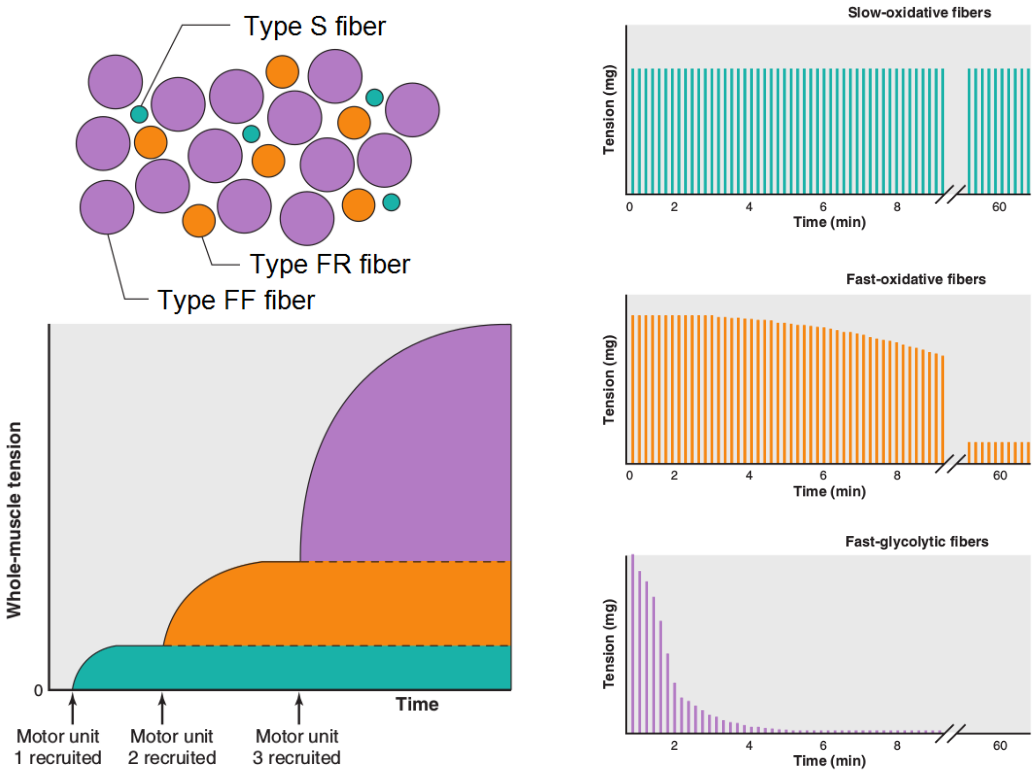

(a) (b)

Figure 1.5: Figure describes characteristics of different types of muscle fibers. In **a)** is a diagram of different muscle fibers in muscle cross section (top), and muscle tension produced by recruitment of different types of muscle fiber (bottom), whereas in **b)** is the illustration of the time interval during which specific muscle fibers can remain tension. It can be noted that type S fibers are activated first, generate low force level, and are resistant to fatigue. On the other hand, type FF fibers are activated last, generate high forces, and develop fatigue fastest. Retrieved from (Widmaier et al., 2003)

to fatigue. If greater force is required, muscle units with higher threshold that are prone to fatigue are activated (Freund et al., 1975; Merletti and Parker, 2004). This was firstly proposed by Henneman et al. in 1965 (Henneman et al., 1965), who state that order of recruitment of motor neurons is based on size principle, that is, neurons with smaller axons are recruited at lower effort levels and with increase in force, larger motoneurons are recruited. Therefore, S type muscle units, which have the smallest motoneurons are recruited first, followed by FR type units, and finally FF units. The recruitment strategy and resistance to fatigue can be seen in figure 1.5.

1.2 Muscle contraction

Skeletal muscles are activated voluntarily by electro-chemical impulses of motor neurons. The process is described in this chapter in summarized version. For more detailed description, the reader is pointed to medical literature (e.g. Widmaier2014).

During the stable state when there are no stimuli, i.e., in the resting state, the interior of the myocyte is at higher electrical potential that the exterior. This difference in potential is usually around 80 mV and it is caused by the higher concentration of positive ions, namely Na+, outside of the sarcolema (Nazmi et al., 2016), as shown in figure 1.6.

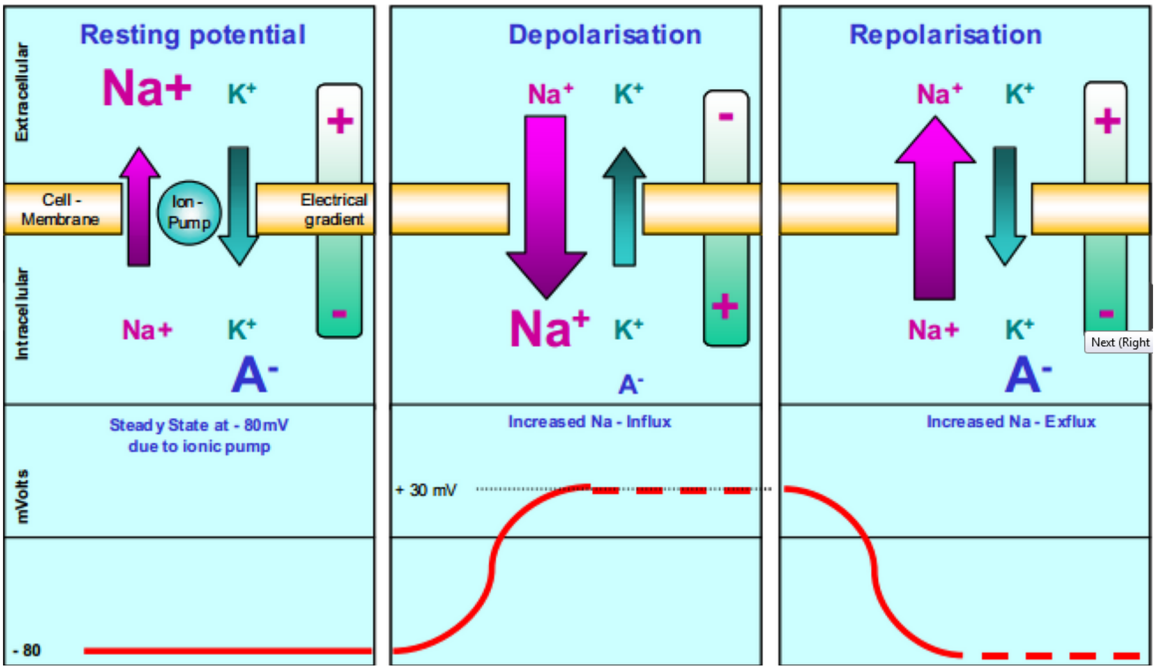

Figure 1.6: Ilustration of depolarization/repolarization of the muscle fiber. Adopted from (Nazmi et al., 2016).

Motor neurons transfer nerve impulses that control the muscle from spinal cord to neuromuscular junction. At the nerve endings, action potentials induce the opening of calcium channels, which enables calcium from extracellular fluid to enter axon terminals and trigger the release of the neurotransmitter *acetylcholine*. Acetylcholine is released to the narrow space between the axon and sarcolema of the myocyte, and causes sodium channels in sarcolema to open and allow the flow of Na+ and K+ ions in both directions. Na+ ions now flow into the myoplasma by diffusion due to higher concentration of Na+ ions outside of the membrane, but because of similar gradient, concentrations of the K+ ions don't change a lot. This process causes depolarization of sarcolema during which the outside potential of the muscle cell is at lower voltage than inside potential by around 30 mV. Depolarization is immediately followed by repolarization, a process during which the electrochemical balance and the resting potential of the cell are restored. It is achieved by flushing the Na+ ions outside of the sarcolema by the *ion pump*. The process can be seen in figures 1.6 and 1.7.

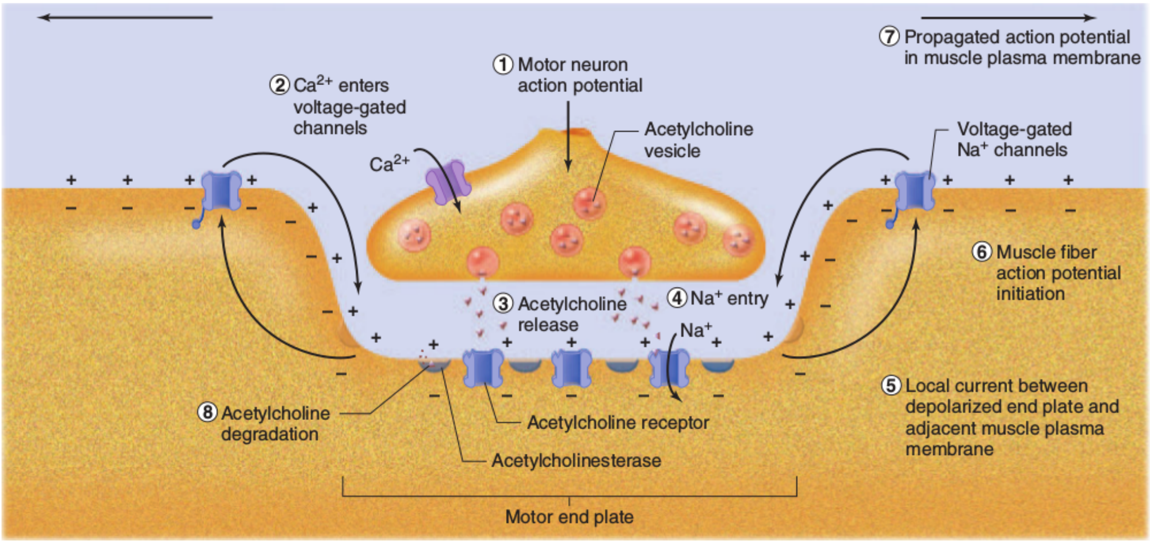

Figure 1.7: Illustration of generation of action potential. Retrieved from (Widmaier et al., 2003).

If the amount of acetylcoline is sufficient for the excitation, depolarization/repolarization wave, that is, action potential, propagates longitudinally from the neuromuscular junction towards the ends of the muscle fiber causing contraction (Henneberg, 1999). Speed of action potential propagation is called *conduction velocity* and typically ranges around 4 m/s.

Detailed analysis of muscle physiology can be found elsewhere (Squire, 1986; Widmaier et al., 2003).

1.3 Muscle fatigue

According to Widmaier et al. (2003), muscle fatigue is a decline in muscle tension as a result of previous contractile activity. It is also characterized by decreased relaxation rate and lower shortening velocity of muscle fibers. Muscle fatigue is a continuous process that starts at the moment when muscle unit activates. If muscle keeps contracting long enough, eventually it will stop contracting because of electro-physiological inability to maintain the contraction. This moment is called the failure point (De Luca, 1984). The failure point depends on many different factors physiological characteristics, but also on the number of muscle fibers and proportion of Type I/Type II muscle fibers. Muscles with higher proportion of Type I fibers do not fatigue easily and recover sooner than type II fibers. However, type II fibers are able to generate higher forces (Kupa et al., 1995).

Factors causing fatigue can be found in the muscle itself, which is *peripheral fatigue*, but can also originate in central nervous system, in which case it is *central fatigue.*

With respect to the source of impairment, the muscle fatigue can be:

Peripheral fatigue

Peripheral fatigue occurs in muscle itself, when because of electro-chemical imbalance muscle contraction is prevented. There are three main sources of peripheral fatigue:

- During sustained contraction, sarcolema of the muscle fibers become acid, and this accidifation lowers the muscle fiber conduction velocity (De Luca, 1984).
- High concentration of K+ ions prevents generation of action potentials in muscle fiber (Widmaier et al., 2003).
- Buildup of adenosine diphosphate, a byproduct of muscle contraction, slows the rate of cross-bridge cycling, affecting the relaxation, and reducing shortening velocity (Widmaier et al., 2003).

Central fatigue

Central fatigue occurs in central nervous system that controls the movement. It is manifested by synchronization of neural spike trains of different motor units. Probably by following the principle that by activating more muscle units simultaneously, total output force of the muscle is higher.

Muscle fatigue changes characteristics of the myoelectric signal. Due to decrease of muscle fiber conduction velocity, caused by peripheral fatigue, but also due to synchronization of firing times caused by central fatigue, there is a shift of energy in frequency spectrum of myoelectric signal towards lower frequency, as shown in figure 1.8 (De Luca, 1984). Another indicator of muscle fatigue is increase of amplitude of surface electromyographic signal. This increase occurs due to two main reasons:

- Tissue between muscle fibers and recording electrodes positioned on the surface of the skin (e.g. fat layers, skin, etc.) have low-pass properties on the propagating electromagnetic wave. Since the power of the propagating wave shifts towards lower frequencies, amplitude of the recorded signal increase.
- Due to synchronization of firing patterns cause by central fatigue, amplitude of recorded sEMG signal increases.

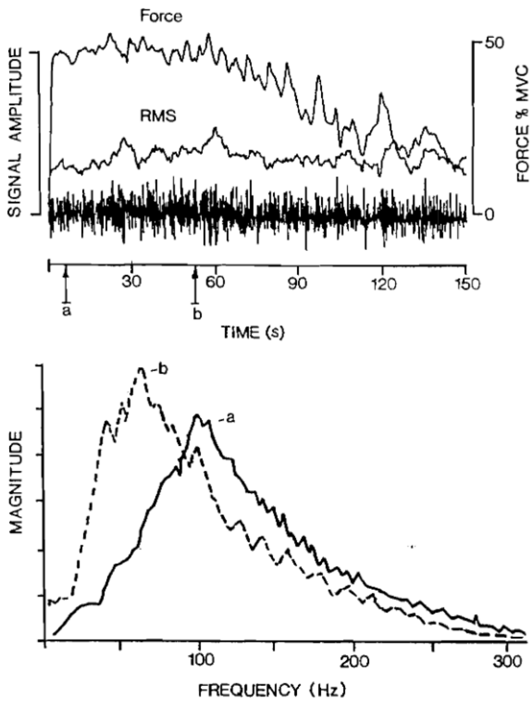

Figure 1.8: Illustration of force and EMG signal recorded during fatiguing exercise (top), and frequency spectra of corresponding EMG signal (bottom) recorded at the beginning of the exercise (a), and at time when force started decreasing (b). Retrieved from (De Luca, 1984).

There are many studies exploiting this changes in sEMG signal to estimate and monitor muscle fatigue. Most of the approaches are based on monitoring frequency characteristics of the signal. One of the simplest measures is number of zero-crossings (Hägg, 1981), but it is very sensitive to noise. Mean and median frequencies are often used in literature (Lindstrom and Magnusson, 1977; Merletti and Lo Conte, 1997; Stulen and De Luca, 1981), but also more advanced time-frequency processing methods (Knaflitz and Bonato, 1999; Cifrek et al., 2000; Georgakis et al., 2003; Srhoj-Egekher et al., 2011).

1.4 Surface electromyography

Muscle unit action potentnial (MUAP) is the combination of action potentials generated by all muscle fibers belonging to that motor unit, whereas myoelectric signal is a superposition of electrical activity (propagating action potentials) produced by all muscle units.

There are two main types of electromyographic measurements:

Surface EMG (sEMG) This is non-invasive type of EMG measurement where electrodes are positioned on the surface of the skin. Two types of electrodes are used: wet electrodes, which are used in combination with conductive gel that provide high signal quality, and dry electrodes, which can be applied directly on the skin. Although wet electrodes are mostly used, signal quality deteriorates during recording because of evaporation of the gel.

Intramuscular EMG (iEMG) This is invasive type of recording which implies insertion of needle or wire electrodes under the skin (Marateb et al., 1999). This type of recording is used for precise measurement of narrow volume, for example couple of muscle fibers. It has high SNR, but causes discomfort in subjects. It It is often used in clinical practice because it can detect abnormal functionality. For example, action potentials of spontaneously contracting single muscle fibers can be measured. These potentials are an important sign of deinnervation, but cannot be recorded using sEMG (Merletti and Parker, 2004).

Although iEMG signal usually has higher quality (in terms of signal-to-noise ratio), it was shown that both approaches provide a similar identification rate of upper-arm motor task (Hargrove et al., 2007). Since sEMG is non-invasive, it is usually preferred method in myocontrol. Moreover, although often narrow volume scope of iEMG can be beneficial, especially in clinical applications regarding activation of single muscle unit, it does not provide information on other parts of the muscle. For that reason, sEMG can be more appropriate because it simultaneously records action potentials of large muscle area. Depending on the application, that can also be a serious drawback because if there are several active muscles in small volume, myoelectric activity of both muscles will be recorded, i.e., there will be *crosstalk* between muscles.

Surface electromyographic signal is the sum of the electrical activity of the muscle fibers recorded on the surface of the skin. From statistical point of view, EMG signal can be considered as a non-stationary stochastic process whose probability density function is the Gaussian function. (De Luca, 1984, 1979). Since muscle fibers are activated by the impulse train of the innervating motor neurons, i.e. neural drive to the muscle, sEMG is the convolution of motor neuron spike trains by the motor unit action potential recorded on the electrodes (Farina et al., 2010, 2014a):

$$sEMG(t) = \sum_{i=1}^{M} \sum_{j=-\infty}^{+\infty} MUAP_i(t)\ \delta(t - t_{i,j}) \tag{1.1}$$

, where M is the number of active motor units, $MUAP_i(t)$ is the action potential waveform of the i^{th} motor unit recorded by the electrodes, and $t_{i,j}$ is the time of the discharge of the i^{th} motor neuron. This model assumes there is no interference and that neuromuscular junction never fails, which is not the case. In the equation, $MUAP_i(t)$ is related to the electrophysiological state of the muscle fiber membranes and conduction properties of the tissue through which the potential propagates, whereas neural information is contained in motor neuron spike trains $\delta(t - t_{i,j})$ (Farina et al., 2014b). With respect to muscle fatigue explained in the previous section, peripheral fatigue affects $MUAP_i(t)$, whereas central fatigue have effect on $\delta(t - t_{i,j})$ term. It is important to notice that following this model, sEMG reflects all motor control information that is present in motor neuron. For that reason, it is more appropriate to extract motor control information carried by motor neurons using sEMG, than directly by invasive measurement of electrical potential of the motor neuron. The advantage of the sEMG is that multiple fibers are activated simultanously, generating bioelectrical signal with relatively high SNR, which can be measured on the surface of the skin. In this context, sEMG can be considered as the amplified neural signal, whereas muscle can be considered as a biological amplifier of nerve activity (Farina et al., 2014a). Origin of sEMG signal can be seen in figure 1.9.

In frequency domain, motor unit action potential spike train provides both the neural and

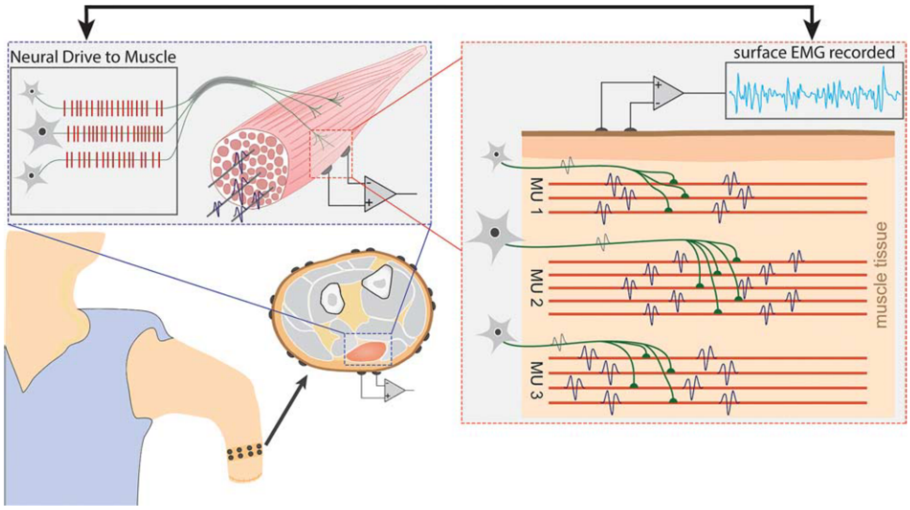

Figure 1.9: sEMG signal is a superposition of motor unit action potentials recorded on the electrodes convoluted by belonging motor neuron spike train. Retrieved from (Farina et al., 2014a).

peripheral information:

$$P_{sEMG}(f) = \sum_{i=1}^{M} P_{ST_i}(f) \left|\Phi_{MUAP_i}(f)\right|^2 \tag{1.2}$$

,where $P_{sEMG}(f)$ is the power spectrum of sEMG signal, $\Phi_{MUAP_i}(f)$ is the Fourier transform of the $MUAP_i$, and $P_{ST_i}(f)$ is the power spectrum of the spike train that innervates it. It is assumed that spike trains are uncorrelated process (Farina et al., 2014a).

In case of constant average discharge rate of spike trains (stationary process), spike train power spectrum can be calculated as:

$$P_{ST_i}(f) = DR_i \left[1 - \left|Q_i(f)\right|^2\right] + DR_i^2 \left|Q_i(f)\right|^2 \sum_{n=-\infty}^{+\infty} \delta(f - nDR_i) \tag{1.3}$$

, where DR_i is the average discharge rate, and $Q_i(f)$ is the Fourier transform of the probability density function of the inter-spike interval variability. The first term in the equation is dominant and equal to DR_i for frequencies greater than 10 - 20 Hz (Lago and Jones, 1977; Farina et al., 2014a). Therefore, the power spectrum of the sEMG signal can be estimated as:

$$P_{sEMG}(f) \approx \sum_{i=1}^{M} DR_i \left|Q_i(f)\right|^2 \tag{1.4}$$

Power of the EMG signal P can be obtained in the frequency domain as:

$$P = \int_0^{+\infty} P_{sEMG}(f)\, df \;\approx\; \sum_{i=1}^{M} DR_i\, E_i \tag{1.5}$$

,where E_i is the energy of $MUAP_i$. It can be noted that the power of sEMG is sum of energies of action potentials of motor units weighted by their discharge rate. When the force of contraction is increased, the power of EMG increases also because of the activation of additional motor units (M increases) and because of the increase of the the average discharge rate of motor neuron action potentials (DR_i increases). When the muscle is fatigued, the conduction velocity of muscle fibers decreases and the power spectrum of muscle fiber action potentials shifts towards lower frequencies, as explained in section 1.3. Due to this effect, energy of MUAPs recorded on the electrodes can increase, leading to increase of sEMG power (E_i increases).

Given the fact that there is large variability between shape, and amplitude of MUAP with respect to electrode position and tissue conduction characteristics, the association between power of the sEMG and the neural drive can also have very high variability, depending on individual subject and muscle (Farina et al., 2014a).

Depending on number of electrodes used for the recording. the following classification exists: single-channel recording in monopolar mode, single channel recording in bipolar mode, recording using linear electrode array, and high-density EMG, as shown in figure 1.10).

In single-channel monopolar recording, a single electrode is positioned over the muscle, whereas the reference electrode is positioned over the place that does not generate electrical activity. On the other hand, single-channel bipolar electrode configuration is most often used, in which signal is a difference of potential between two electrodes. These configuration is traditionally preferred because of the lower interference and higher signal-to-noise ration (Merletti and Parker, 2004). General recommendation is that the inter-electrode distance is around 20 cm (Hermens

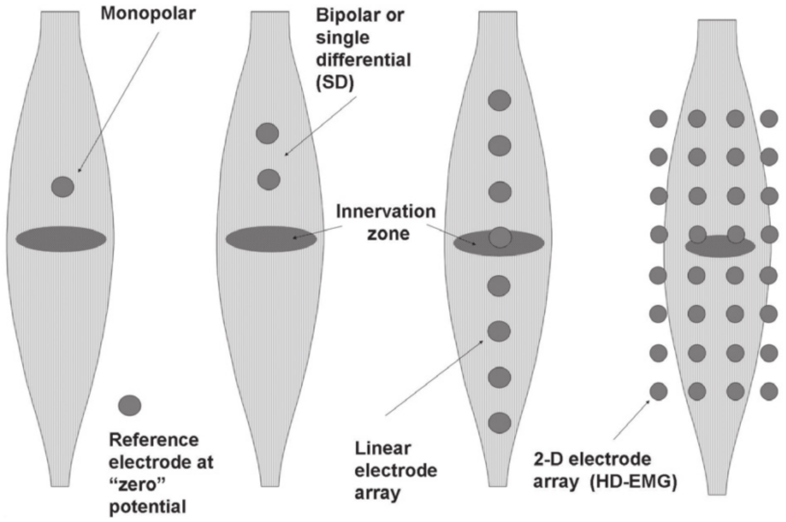

Figure 1.10: Four types of recording surface EMG signal: monopolar, bipolar, linear electrode array, HD-EMG. Figure was modified from (Merletti et al., 2010).

and Freriks, 1999), but the optimal distance depends on many factors, as briefly explained in (Hakonen et al., 2015). For both monopolar and bipolar single channel recordings it is recommended that the electrodes are positioned between innervation zone and tendon. Exact recommendations can be found in the findings of the SENIAM project Hermens and Freriks (1999).

Linear electrode array consists of multiple electrodes positioned at equal distance along the muscle line, folowing the direction of propagation of action potentials. Measurements recorded using this type of electrodes provide more information on the muscle. For example, it can be used for estimation of conduction velocity, as shown is figure 1.11 (Merletti and Parker, 2004).

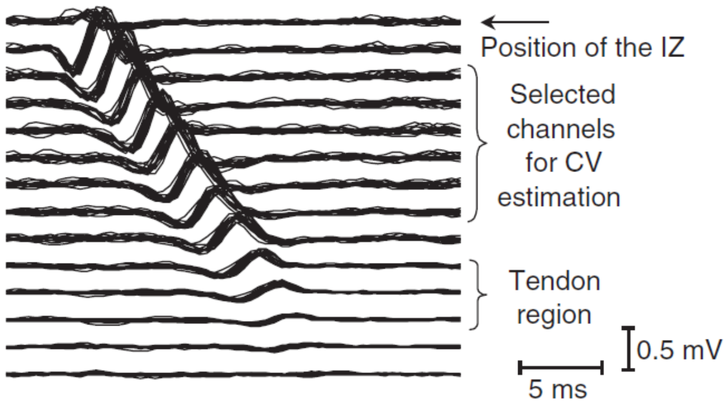

Figure 1.11: Estimating conduction velocity using averaged MUAPs recorded using linear electrode array. Figure was retrieved from (Merletti and Parker, 2004).

Technological advancement of EMG acquisition systems enables use of high-density electromyography (HD-EMG) (Zwarts et al., 2004). Using an array of closely spaced electrodes organized in a quadrature grid, multiple EMG channels are recorded over the wide area of the muscle. Electrodes used for HD-EMG recording can be seen in figure 1.12. This type of recording is more reliable because it can record activations in different parts of the muscle and increase redundancy. HD-EMG is the only EMG recording approach that allows insights into spatial distribution of motor units in a muscle. By observing the amplitude or intensity of signals recorded in different channels, it is possible to analyze how different muscle regions activate depending on joint position (Vieira et al., 2010), contraction level (Holtermann et al., 2005), and duration of movement and fatigue (Tucker et al., 2009; Staudenmann et al., 2014). Moreover, Zwartz et al. pointed out that single channel EMG disregards important spatial aspects of MUAP propagation, which are essential for the force-generating capacity of the muscle, and, if not well addressed, can lead to incorrect conclusions (Zwarts and Stegeman, 2003). Moreover, since muscles do not activate homogeneously, single bipolar channel EMG has some serious drawbacks, which can be overcome by using 2D electrode arrays.

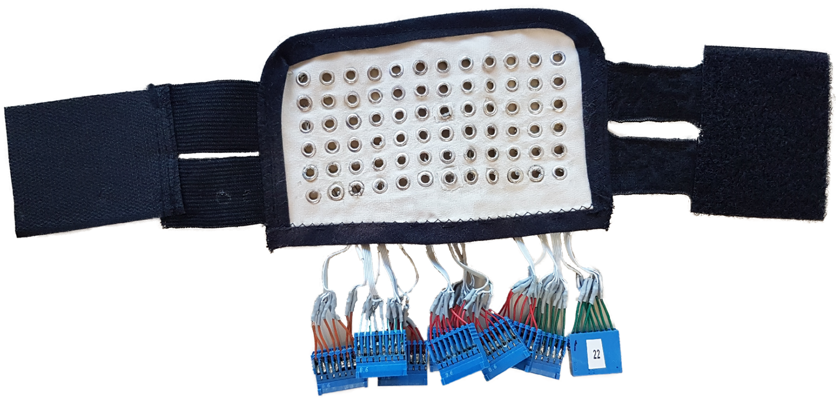

Figure 1.12: The figure represents HD-EMG electrode that was used for recording of database used in this Thesis.

In addition, activation of individual motor units, i.e. individual motor neuron spike train, can be extracted from the HD-EMG recordings using Blind Source Separation methods (Holobar and Zazula, 2007; Holobar et al., 2010), which can be a valuable information in force estimation because motor unit recruitment and firing frequency depend primarily on force level (Merletti and Parker, 2004). Several authors have used this approach instead of the traditional one based on intramuscular (invasive) EMG. One of the obvious advantages of this method is that is safe and not painful, although it has not been implemented in clinical practice yet. Using this technique, Holobar et al. (Holobar et al., 2010) were able to extract 6 to 7 motor units starting from contractions at 5% MVC and up to 20% MVC with associated discharge rates between 10 pps and 12 pps. However, one of the current limitations is that the intensity of isometric contraction must remain constant during the measurement.

HD-EMG recordings also allow calculation of two-dimensional activation maps where intensity of each pixel represents the intensity of a corresponding EMG channel (see figure 1.13). Consequently, the information on spatial distribution of EMG intensity over the muscle is provided. Recent studies show that changes in spatial activation pattern are related to duration of movement and fatigue (Tucker et al., 2009; Staudenmann et al., 2014), position of joint (Vieira et al., 2010) and the level of contraction (Holtermann et al., 2005).

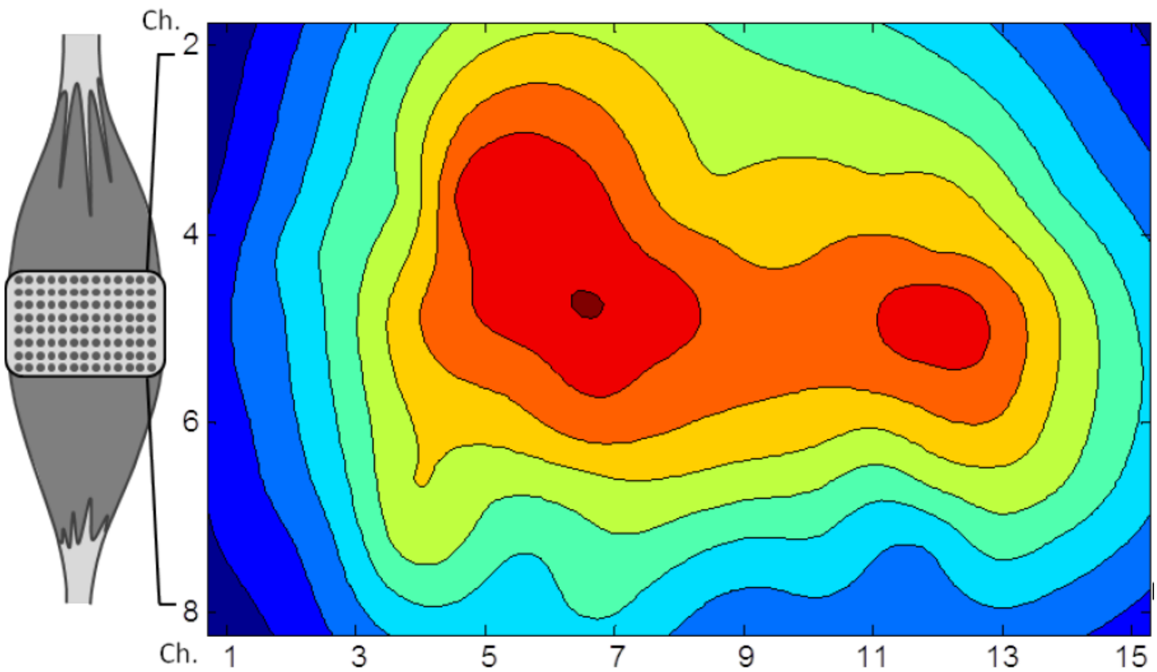

Figure 1.13: The figure represents the HD-EMG activation map recorded on the biceps brachii muscle during flexion. Distinct activation of the two heads can be noticed in the map. Modified from (Rojas-Martínez, 2012)

These HD-EMG activation maps can be also used to determine multiple innervation zones (Marateb et al., 2016), but it was also proven that this spatial characteristics of HD-EMG change depending on the task, but also depending on the force the subject is applying, and form repeatable muscle activation pattern that can be used in identification of motion intention (Rojas-Martínez et al., 2012).

However, HD-EMG can be corrupted by low quality channels, which are a common issue in measurements due to well-known artifacts, such as: electrode displacement, bad electrical contact between skin and the electrode, movement of cables, electromagnetic interference, etc. (Clancy et al., 2002). Affected channels differentiate themselves in amplitude and spectral content. To cope with this problem, authors in (Rojas-Martínez et al., 2012) developed an expert system for detection, removal and interpolation of HD-EMG channels corrupted by artifacts. On the other hand, Ghaderi and Marateb (Ghaderi and Marateb, 2017) used image inpainting and surface reconstruction methods to reconstruct the corrupted activation map.

1.5 Task identification using pattern recognition

Given the one to one relationship between the neural commands and the activation of motor units in the muscles, surface electromyography (sEMG) has been used for more than a half of century as a noninvasive and natural way of extracting motor control information for identification of motion intention. Such information is used in numerous applications in rehabilitation engineering, e.g., prosthetics (Li et al., 2010; Young et al., 2013; Stango et al., 2015), exoskeletons (Vaca Benitez et al., 2013) and rehabilitation robots (Dipietro et al., 2005; Marchal-Crespo and Reinkensmeyer, 2009).

Ideally, an identification system should fulfill the following criteria (Farina et al., 2014a):

- Intuitive control: simultaneous and proportional
- Insensitive to changes in electrode - skin impedance,
- Adaptive to changes during the use, i.e. fatigue, electrode-skin impedance change due to sweating and drying of conductive gel
- Insensitive to precise position of electrodes
- Fast and easy training procedure (ideally none)

- Real time identification, i.e. time delay less than 300 ms (Oskoei and Hu, 2007)
- Low computation complexity which enables implementation in battery-powered device

In most of the commercial prosthesis (Parker and Scott, 1986), sEMG of two muscles is recorded. In this simple scheme a single Degree-of-Freedom (DOF) can be controlled: the EMG amplitude of one muscle controls the output of one direction, whereas the EMG amplitude of the other muscle controls the other direction. If prosthesis needs to operate in multiple DOFs, a subject needs to switch between currently active DOF either by co-contraction or by pressing a switch button. In any case, the method is not intuitive nor efficient for the user (Farina et al., 2014a).

Pattern recognition is an alternative to conventional control algorithms and has been extensively used in research institutions during last decades (Hakonen et al., 2015; Farina et al., 2014a). The prerequisite of using pattern recognition for task identification is the presence of a pattern that can be extracted from the EMG signal. Major advancement over conventional switching myocontrol is the possibility of instant selection of one of predefined movements.

However, although pattern recognition improves the possibilities of extraction of motion intention, it has serious limitations. Therefore, there is still a large gap between use of pattern recognition in research and in practice in rehabilitation institutes and in users' homes (Jiang et al., 2012). Pattern recognition approach does not support proportional and simultaneous control for multiple motor tasks. Therefore, consecutive tasks need to be performed sequentially. This type of control prevents the user from achieving a fluid movement, but also demands planning of movement execution. There have been solutions proposed in literature that enable simultaneous controls over multiple degrees of freedom. For example, Young et al. (Young et al., 2013) propose system of parallel classifiers that use conditional probabilities to separate between combination of tasks. On the other hand, there are also publications proposing solutions for proportional control. Fougner et al. prepared a review on the topic (Fougner et al., 2012). The main idea behind this technology is that the muscle force can be estimated using the EMG signal (Staudenmann et al., 2010).

On the other hand, one of the disadvantages of pattern recognition is the fact that in spite of the high accuracy, an error could lead to the completely unwanted task. Furthermore, although identification rate is usually very high during the stationary task, errors often occur during transition between tasks. This problems can be partially prevented by employing the e.g. majority voting principle (Englehart and Hudgins, 2003), or decision-based velocity ramp that attenuates the velocity of a movement after the change of a task (Simon et al., 2011).

Although crosstalk is usually considered as a negative interference in electromyography, if it is consistent and repeatable, some authors argue that it can provide a discriminative power for task identification (Farina et al., 2014a). However, for some approaches it has a negative influence (He et al., 2015). To resolve this issue, source separation methods can be used to separate EMG activity of adjacent muscles (Farina et al., 2004; Holobar and Farina, 2014). This can be a powerful tool in task identification (Naik et al., 2007), because it could separate contributions of individual muscles in the myoelectric signal, and, therefore, minimize crosstalk effect from nearby muscles. Consequently, extracted features would characterize only the target muscles.

According to Oskoei et al. pattern-recognition-based task identification approach includes four main modules (Oskoei and Hu, 2007):

Data segmentation:

Comprises various techniques and methods that are used to handle data before feature extraction. Recording must be divided in time segments on which identification will be performed. Selection of duration of time segment has effect on the identification. Features calculated on wider segments usually have lower variability and, consequently, higher repeatability and stronger pattern, which increases identification rate. On the other hand, the output of the classifier should be as fast as possible in order to be used in real time. Therefore, the shorter the window, the shorter the response time will be. General recommendation is that the delay should be less than 300 ms (Oskoei and Hu, 2007; Englehart and Hudgins, 2003).

Feature extraction:

This module computes and presents preselected features for a classifier. Features, instead of raw signals, are fed into a classifier to improve classification efficiency. Selection or extraction features is one of the most critical stages in myoelectric control design.

Classification:

A classification module recognizes signal patterns, and classifies them into predefined categories. Due to the complexity of biological signals, and the influence of physiological and physical conditions, the classifier should be adequately robust.

Controller:

Generates output commands based on signal patterns and control schemes. Post-processing methods, such as majority voting, which are often applied after classification to eliminate destructive jumps and make a smooth output, are included in this module too.

Many studies agree that selection of pattern recognition technique does not have a big influence on the task identification (Hakonen et al., 2015). Therefore, simple and fast classifiers are preferred. Linear discriminant analysis has become the 'gold standard' in the field of myoelectric control because of this properties (Tkach et al., 2010; Li et al., 2014; Hakonen et al., 2015). Although this classifier assumes multivariate normal distribution of classes, experiments proved that it performs well if when normality assumption is not met (Grouven et al., 1996). Features, on the other hand, have a major influence on the identification results (Englehart et al., 1999; Tkach et al., 2010). Therefore, there are many features proposed in the literature focused on improving rate of identification of motion intention:

Time domain features:

Mean absolute value (Hudgins et al., 1993), integrated EMG (Park and Lee, 1998), variance (Park and Lee, 1998; Zardoshti-Kermani et al., 1995), root mean square (Farrell and Weir, 2008), waveform length (Hudgins et al., 1993), zero crossing (Hudgins et al., 1993), log detector (Tkach et al., 2010), Wilson amplitude (Zardoshti-Kermani et al., 1995), slope sign change (Hudgins et al., 1993), autoregressive coefficients (Hargrove et al., 2007), cepstral coefficients (Park and Lee, 1998), mean absolute value slope (Phinyomark et al., 2012a), histogram of EMG (Phinyomark et al., 2012a; Zardoshti-Kermani et al., 1995)

Frequency domain features:

Mean frequency (Phinyomark et al., 2012b), median frequency (Phinyomark et al., 2012b), modified mean frequency (Phinyomark et al., 2009)

Time-frequency domain features:

Short time Fourier transform (Englehart et al., 2003, 2001), continuous wavelet transform (Englehart et al., 2003, 2001), discrete wavelet transform (Englehart et al., 2003), stationary wavelet transform (Englehart et al., 2003), wavelet packet transform (Englehart et al., 2003, 2001; Chu et al., 2006)

Spatial domain features:

Experimental variogram (Stango et al., 2015), center of gravity (Rojas-Martínez et al., 2012, 2013)

Time domain features are commonly used because they achieve high identification accuracy and are computationally efficient (Hakonen et al., 2015).

Since spatial distribution contains a lot of information on the muscle, it is acknowledged as a valuable feature in identification of motion intention (Stango et al., 2015; Hakonen et al., 2015; Rojas-Martínez et al., 2013). For example, Stango et al. (Stango et al., 2015) used spatial characteristics of HD-EMG recording of the forearm muscles to identify 8 hand and wrist tasks (4 degrees of freedom). They fed support vector machine classifier with a statistical measure of spatial correlation, i.e. variogram and achieved high identification results (95% accuracy). Furthermore, they proved that proposed spatial features are robust to electrode shift.

Most of pattern recognition identification methods are subject-specific. They usually achieve very high identification results, but require time consuming training procedure for every patient individually. This could be avoided by building a single identifier for a group of patients, i.e. group-specific identifier. However, inter-subject variability is a big concern in design of a group-specific pattern recognition-based identifier. Individuals differ from each other in a lot of physiological parameters, e.g., conductivity of subcuntaneous tissue, and limb dimension. Nevertheless, by comparing HD-EMG activation maps between normal subjects it has been shown that inter-subject activation patterns exists for different tasks and levels of contraction (Rojas-Martínez et al., 2012).

In (Rojas-Martínez et al., 2013) authors demonstrate that by using intensity and spatial features extracted from activation maps it is possible to construct an inter-subject identification method based on LDA classifier not only for different tasks, but also for different effort levels. Authors reported that in healthy subjects identification performance improves by adding spatial features in the identification, which proves that spatial distribution is less sensitive to inter-subject variability. They achieved sensitivity higher than 75% for identification of four upper-limb tasks at three different effort levels and more than 90% sensitivity when identifying only four tasks and no effort level. Also, they report higher classification results when using classification in two steps (in first step task is classified, and in the second step level of effort), rather than a single step classification.

1.6 Application to patients with neuromuscular impairment

Physical injury to the brain, spinal cord, or nerves, is usually the cause of neurological disorders. According to World Health Organization, each year there are 500 000 spinal cord injuries and 15 million strokes (of which 5 million result with death and 5 million with permanent disability) every year. Furthermore, number of people who are older than 60 years will increase to 22% of the world population by 2050 and will count 2 billion people. Unfortunately, in affected patients motor control can be impaired as a result of damaged nerves and they often suffer from uncoordinated movements, lack of force, and spasticity. On the other hand, stroke is a serious life-threatening condition that occurs when the blood supply to the brain is interrupted, resulting in severe disability among survivors. Brain damage due to stroke can affect important areas that control everything we do, including how we move different parts of our body. Common manifestations of upper extremity motor impairment include muscle weakness, impaired motor control, and changes in muscle tone are common manifestation of upper extremity motor impairment. These impairments induce disabilities in common daily life tasks like reaching and holding objects. During recovery process, rehabilitation robots that stimulate neuroplasticity are commonly used (Vaca Benitez et al., 2013; Dipietro et al., 2005; Marchal-Crespo and Reinkensmeyer, 2009).

Patients can still have uncoordinated movements, and lack of force, or, in more difficult cases, they can weakly activate their muscles, but cannot perform the movement. If their motion intention could be extracted in real time, it would allow them to control assistive devices and maximize the benefits of robotic-aided therapies where it has been proved that the active participation improves the medical condition of the patient (Hogan et al., 2006).

It was already shown that intensity-related and task-specific activation patterns exist in patients with neurological disorders and that motion intention can be extracted from EMG. In other words, movement that patient is trying to perform can be predicted using the recorded myoelectric activity. Liu and Zhou were able to successfully perform identification of tasks using time domain and autoregressive model features in patients with incomplete spinal cord injury (Liu and Zhou, 2013), whereas Zhang and Zhou identified tasks in patients with stroke using a similar feature set (Zhang and Zhou, 2012).

After the neurological disorder, rehabilitation treatment should start as soon as possible, only days after injury in stroke, whereas in case of spinal cord injury, after the inflammation. Early interventions can achieve incredible results and patients can either regain control of limbs, which is known as *true recovery*, or can learn new compensatory movements, which is called *restitution*.

In spite the correct neuromuscular activation, patients sometimes cannot achieve movement because of insufficient contraction force, or spasticity (Liu et al., 2016). These patients have good chance of recovery, but therapists are often unaware of their state. On the other hand, rehabilitation robots are mostly based on force and inertia, and, therefore, cannot be of assistance either. Since this patients have the ability to generate EMG signals, they could control a rehabilitation robot and maximize their chance of recovery by individualizing rehabilitation.

1.7 Doctoral thesis overview

This Doctoral Thesis is presented as the compendium of three publications. The topic of the Thesis is the analysis of muscular patterns of upper-limb muscles during isomeric contractions and its relationship to incomplete spinal cord injury. Furthermore, method for the identification of motion intention is developed base on pattern recognition approach and muscle co-activation patterns.

The Doctoral Thesis is organized by chapters as follows:

- **Chapter 2: Problem statement**

This chapter states the problem and provides the objectives of Doctoral Thesis.

- **Chapter 3: Spatial distribution of HD-EMG improves identification of task and force in patients with incomplete spinal cord injury**

  This chapter represents the first publication of the compendium of publications. Using spatial distribution of myoelectric intensity task identification was performed on patients with incomplete spinal cord injury. This work proves the positive contribution of spatial features in pattern recognition technique of identification of motor tasks. Not only that the identification rate increases, but the features show resilience to slow time dependent changes in the myoelectric signal, such as fatigue and drying of electrolytic gel.

- **Chapter 4: Prediction of isometric motor tasks and effort levels based on high-density EMG in patients with incomplete spinal cord injury**

  In this publication, the similarity of intensity and spatial distribution of intensity was investigated between patients with incomplete spinal cord injury. The results show that the repeatable pattern exists between different patients and, moreover, for the patients with similar level of injury this patterns are more similar.

- **Chapter 5: A Novel Spatial Feature for the Identification of Motor Tasks Using High-Density Electromyography**

  This chapter summarizes the third publication of the compendium. The novel feature was designed for task identification. It is based on probability density function of HD-EMG activation maps. Classifier based on this new feature show higher identification rate, as well as fidelity to fatigue.

- **Chapter 6: Conclusions**

  In the last chapter, the conclusions and main contributions of the Thesis are provided. Also, the guidelines for the future work are stated, as well as list of publications derived from the Thesis.

Chapter 2

Problem statement

Extraction of information on motor task intention can be used in many different application from assistive devices, prosthetics, and rehabilitation robots to leisure and gaming equipment. This information can be extracted at any point of the system for motor control. The central nervous system is organized in multiple levels, from simple connections between cells to coordinated cell populations, building a complex architecture of interconnected brain regions, including the centers for motor control. All this brain activity is summed together and its electromagnetic field can be measured on the scalp surface (EEG). In that case, the system is brain-computer interface (BCI). Although this approach is being extensively researched and the possibilities and achievements are rising rapidly, it is not an easy task. The problem is that activity of entire brain is superimposed to the motor control activity. On the other hand, EMG is electrical activity of many muscle units that carry similar information. The ration of power of useful signal, compared to interference of other sources is much higher in EMG recordings. Moreover, by recording myoelectrical activity over muscle surface with high spatial sampling (HD-EMG), even higher SNR can be achieved and more information can be extracted. Therefore, this Doctoral Thesis investigates the possibilities of extraction of motor control information from multichannel sEMG during voluntary contractions.

2.1 Motivation

Voluntary movements are achieved by the contraction of skeletal muscles controlled by the Central and Peripheral Nervous system. The contraction is initiated by the release of a neurotransmitter that promotes a reaction in the walls of the muscular fiber, producing a biopotential known as Motor Unit Action Potential (MUAP) that travels from the neuromuscular junction to the tendons. The surface electromyographic signal records the continuous activation of such potentials over the surface of the skin and constitutes a valuable tool for the diagnosis, monitoring and clinical research of muscular disorders. Moreover, the use of electrode arrays facilitate the investigation of the peripheral properties of the active Motor Units such as: conduction velocity and fatigue (Soares et al., 2015); anatomical characteristics in terms of location of the innervation zones (Beck et al., 2012), the spatial composition of the muscle, that is, muscle compartmentalization (Vieira et al., 2010); and change in spatial distribution of MUAPs with exercise and pain (Madeleine et al., 2006). This last property of the muscles has proven to be very useful to infer motion intention not only regarding the direction of the movement but also its power (Rojas-Martínez et al., 2013).

HD-EMG enables measuring of valuable information about muscle unit recruitment: muscle fiber conduction velocity, location of the innervation zones, estimation of muscle fatigue, and estimation of number, type and the spatial distribution of muscle fibers (Marateb et al., 2016). The advantages of the HD-EMG lie in the large amount of recorded information, which enables minimizing the effect of electrodes shift and allows choosing an appropriate subset of channels for further analysis.

In this thesis muscle co-activation patterns will be analyzed both in healthy subjects, but also in patients with incomplete spinal cord injury. Spinal cord injury is a neurologically disabling disease like the stroke. In these types of neuromuscular impairments, patients often have residual motor capabilities and can weakly activate their muscles. However, although their muscle is contracting and generating myoelectrical activity, their contraction sometimes is not strong enough to generate joint movement. In this situation, it is likely that the rehabilitation will not be successful and patient could be advised to start developing compensatory movements to replace the lost functionality. Moreover, rehabilitation robots are widely used in this type of rehabilitation care. However, robots most often have only force sensors and can adjust the trajectory depending on the force that patient is producing in order to assist/resist his efforts. Although it was proven that rehabilitation robots have positive effect on the therapy, their effect on the rehabilitation could be greatly improved if the robots would adjust the force and trajectory based on the HD-EMG myocontrol system connected in the feedback loop. It was already proven that simply moving patient's limb along a set trajectory has minimal effect on the outcome of the therapy and that therapy can be greatly improved if the patient is actively trying to achieve a movement. Therefore, personalize therapy system that responds to patient's movement intention could greatly improve the therapy.

To achieve the accurate identification of motion intention using pattern recognition, repeatable co-activation pattern should be present in the patients with neurologically disabling diseases. Therefore, reproducibility of specific muscular activation patterns will be investigated in patients with incomplete spinal cord injury during four isometric tasks of the upper limb, paying close attention to the spatial activation patterns. Moreover, activation pattern will also be analyzed during different levels of effort.

The measure of pattern reproducibility can be evaluated using pattern recognition classification in task identification. If the features extracted from the HD-EMG signal form a distinct pattern for each of the tasks, and if patterns for different tasks are different, identification results will be high. Recognizable and distinct patterns will yield a high identification results.

Task identification using pattern recognition is classification of recorded EMG signal segments into one of predefined classes based on the characteristics of the recorded EMG signal. These extracted features should ideally form a repeatable and distinct pattern for each class, but different between classes. The main drawback of this method is that only one movement can be activated at the time. Any task that requires more than one DoF must be performed sequentially. However, several authors recently proposed solutions which enable simultaneous control (Young et al., 2013; Kamavuako et al., 2013; Baker et al., 2010). A variety of classifiers (e.g. hidden Markov model, support vector machine, artificial neural network, fuzzy logic and linear discriminant analysis) (Oskoei and Hu, 2007) has been used in myocontrol research. Nevertheless, multiple authors agree that the identification does not significantly depend on the classifier type (Hargrove et al., 2007; Zhang and Zhou, 2012; Hakonen et al., 2015). Therefore, simple and easy to train classifiers like linear discriminant analysis are preferred (Li et al., 2010; Englehart et al., 1999; Tkach et al., 2010; Li et al., 2014; Hakonen et al., 2015). On the other hand, finding an appropriate set of features is challenging (Englehart et al., 1999; Tkach et al., 2010; Liu and Zhou, 2013).

In this work, linear discriminant analysis and support vector machine will be used as pattern recognition classifiers. LDA is a computationally simple and efficient classifier with linear decision boundary and it is based on the Bayesian equation. It is a *parametric classifier*, i.e., it estimates statistical probability of classes by estimating the probability density function of each class from the available data, which is not a simple task and can often be erroneous. On the other hand, SVM is nowadays known as a very powerful classifier with a lot of different applications. The big advantage over LDA is the fact that it is a *non-parametric* classifier. The model is not obtained using assumptions of the form of the class density function and estimation of it's parameters, which is inevitably erroneous. Instead, SVM forms the decision boundary using the samples (not their density estimates) by maximizing the distance between samples and the boundary. This was the idea Vladimir Vapnik, the inventor of this method stood for. It is better to try to solve the problem directly and simply, without many intermediate steps that can often be complicated and inaccurate. Detailed explanation and the working principle of the classifiers is provided in the appendix A.

Challenges in pattern recognition in electromyography are electrode shift (Hargrove et al., 2008; Young et al., 2011), change in arm posture (Fougner et al., 2011), slow time dependent changes (Farina et al., 2014a) such as fatigue (Tkach et al., 2010), and change in electrode-skin impedance (Clancy et al., 2002). In this work, analysis will be performed on highly controlled isometric tasks. Patients limb will be held in place using the mechanical brace, and no movement will be possible. Therefore, effects accounted for limb movement, that is, electrode shift and change in arm posture will be minimal. In this environment, research will only be focused on slow time-dependent changes like fatigue.

2.2 Objectives

Main objective

This Doctoral Thesis addresses the problem of extraction of information from muscular patterns obtained from multichannel surface electromyography and associated with different motor tasks. The aim of the thesis is to analyze the muscular pattern of upper-limb muscles during isomeric contractions and its relationship to neuromuscular disorders, particularly to incomplete spinal cord injury. This information can be useful for the identification of motion intention, i.e. identification of intended motor task and force based on EMG and could provide a control signal to interfaces like exoskeletons or rehabilitation robots, particularly for stroke or other patients with neuromuscular disorders.

Specific objectives

To achieve the main objective, this thesis strives for the following specific objectives:

I To investigate muscle co-activation patterns extracted from multichannel sEMG in patients with incomplete spinal cord injury during isometric contractions. Repeatability of the patterns will be evaluated for different motor tasks, but also for different effort levels. Patterns in intensity and in spatial domain will be evaluated.

II To search for the similarity in multichannel EMG activation patterns between patients with incomplete spinal cord injury using pattern recognition

III To develop a novel pattern recognition-based procedure for identification of task and force of isometric contractions. Special attention will be paid to features related to spatial distribution of myoelectric intensity.

IV To test stability and robustness of extracted features regarding physiological and non-physiological changes which are consequences of long-term contractions (i.e. myoelectric fatigue and gel drying).

V To publish the obtained results and conclusions in high-impact journals and conferences.

2.3 Thesis framework

This thesis and the published articles that provide its content as a compendium were developed in the *Department of Automatic Control (ESAII)* of the *Universitat Politècnica de Catalunya (UPC)* under the framework of the brain research line of the *BIOsignal Analysis for Rehabilitation and Therapy Research Group (BIOART)*, which belongs to the *Biomedical Signals and Systems* division of the *Biomedical Engineering Research Centre (CREB)* of UPC that belongs to the Biomedical Research Networking Center in Bioengineering, Biomaterials and Nanomedicine (CIBER-BBN). The research was done with the collaboration of the Institut Guttman in Badalona (Spain) and the Laboratory of Engineering of Neuromuscular System and Motor Rehabilitation at the Politecnico di Torino.

Furthermore, this work has been supported by multiple funding projects:

1. Ayudas para la contratación de personal investigador novel (FI-DGR 2014). *Agencia de Gestión de Ayudas Universitarias y de Investigación (AGAUR) - Generalitat de Catalunya.*
2. Sistemas multicanal de análisis y sensorización para rehabilitación y monitorización clínica. (DPI2011-22680) *Ministerio de Economia, Industria y Competitividad (MINECO)*
3. Design of methods for assessing processes of neurological and neuromuscular decline associated with aging. (DPI201459049R) *Ministerio de Economia, Industria y Competitividad (MINECO)*

Chapter 3

Conclusion

3.1 Summary

Task identification and movement estimation based on EMG are very popular topics involving different areas in machine learning and, particularly, pattern recognition with many possible applications in assistive and rehabilitation devices. The emergence of high-density EMG (HD-EMG) opened new possibilities for extracting neural information and it has been reported that spatial distribution of HD-EMG intensity is a valuable feature in identification of isometric tasks.

This Doctoral thesis investigates further the spatial muscle co-activation patterns of myoelectric activity extracted from the HD-EMG activation maps. HD-EMG was measured on five muscles of forearm and upper arm in monopolar configuration. Measurements were performed on the group of healthy subjects and on the group of patients with incomplete spinal cord injury.

In the chapters 3 and 4, co-activation patterns of patients with incomplete spinal cord injury were analyzed by the means of pattern-recognition-based identification of task and effort level. In chapter 3, co-activation patterns were analyzed for each patient individually, whereas in chapter 4, co-activation patterns were analyzed within the group of patients. In spite the great diversity between different patients and their levels and types of injury, similarities between activation patterns were found not only in intensity of myoelectric signal, but also in spatial distribution.

In the chapter 5, novel feature for task identification was proposed. The feature is based on spatial distribution of myoelectric activity recorded by HD-EMG. This new feature was evaluated in identification of task and identification of task and effort level in healthy subjects. The evaluation was performed for each subject individually.

3.2 Main conclusions

In chapter 3, intensity activation maps were calculated for each muscle and different features were extracted: the average intensity of an HD-EMG map, and the center of gravity of an HD-EMG maps. Using the extracted feature sets, a successful patient-specific task identification method was designed. It is capable to estimate with high accuracy not only the motor task, but also the force. This implies that patients with incomplete spinal cord injury have repeatable co-activation muscular pattern not only in intensity, but also in spatial distribution of intensity over the muscle. Moreover, the results lead to the conclusion that spatial distribution of myoelectric activity has significant and discriminative power in classification. Furthermore, adding information on spatial distribution of myoelectric intensity improves not only identification result, but also resilience to fatigue and time effect.

Furthermore, in chapter 4 it was discovered that the repeatable patterns in intensity and spatial distribution exist not only for each patient individually, but the pattern exist for the entire group of patient. To demonstrate the existence of distinguishable group-specific patterns in HD-EMG, the identification of different tasks was performed, where classifier was not trained exclusively using the samples of a single patient, but it was trained using the samples of all patients, and tested using the samples of all patients, i.e., group-specific classifier was designed. The existence of the patterns is an interesting result because there is a high level of variability between patients due to the nature of the injury. Co-activation patterns were found not only between different tasks, but also between different effort levels. Group-specific identification of motion intention in patients with neuromuscular impairment could potentially improve the translation of pattern recognition techniques to clinical practice. Also, the results show that the similarity is greater between patients with similar level of lesion. This could also have an interesting implication in translation to the clinical practice because patients with the similar level of injury could be able to use the same assisitive/rehabilitation devices with greater ease.

Finally, in chapter 5, a novel feature for identification of task and effort level was designed. It is based on the locations of local maxima of the probability density function of HD-EMG activation maps. The feature was tested on the population of healthy subjects in subject-specific approach, that is, classifier was trained for each subject individually. The feature yields higher identification indices compared to the more classical features, especially in task identification at very low effort level. By analyzing the influence of fatigue and other time-dependent changes (e.g. drying of conductive gel) on identification, novel feature had a very good performance. Since the goal of this study was to analyze different feature sets rather than classification methods, LDA was utilized given that this method is the most commonly used, and is generally recommended for myoelectric interfaces (Hakonen et al., 2015).

The proposed motor task identification method based on spatial information of myoelectric distribution could contribute to the human-machine interface technology. There are many possible applications for this type of technology, for example computer games, exoskeletons, automatic wheelchairs, rehabilitation robots, prostheses, etc. Nowadays, field of brain-computer interface (BCI) technology is advancing very fast with high investments of leading global corporations. However, non-invasive BCI is still an open problem with low output rate, which can be greatly improved by using EMG-based identification of motor intention. Müller-Putz et al. (Muller-Putz et al., 2015) suggest non-invasive hybrid brain-computer interfaces (hybrid BCI) designed as EEG-based system, supplemented with other biological and mechanical signals. Joining EEG and EMG recordings in identification of task intention significantly improves the accuracy of individual EEG or EMG system. EMG usually has higher SNR ratio than EEG and it is widely used in the identification of the motion intention, however, it is prone to malfunction due to fatigue. When fatigue occurs, the supplemented EEG input keeps the identification stable, and increases the robustness of the system. Thus, advances in obtaining methods more robust to fatigue or time effect are very interesting.

Some patients with neuromuscular impairment can weakly activate their muscles, but insufficiently to generate a movement. In these patients, as well as in patients that can generate only weak movements, HD-EMG maps can still be generated and used in identification of motion intention, as demonstrated in this study. This approach could supplement the existing BCI or inertial sensors based prostheses and result in a device with a better performance. For example, Rohm et al. (Rohm et al., 2013) performed a very interesting study with a single SCI patient. Their neuroprosthesis consisted of a functional electrical stimulation of the forearm and upper arm muscles, and a semiactive elbow orthosis. Using BCI and a shoulder joystick, the patient was able to perform complex hand and elbow tasks from everyday life (e.g. eating an ice cream cone). The reported performance of that study was 70%, which was remarkable considering the fact that the patient did not have any control over involved muscles. However, performance of similar patients could be increased using hybrid BCI if myoelectric activation exists.

Density function from which modes were extracted represents RMS activation maps of the HD-EMG. Although the feature proved to be useful, by calculating RMS value, the information is partially lost. Therefore, the modes, or other statistical measures of the raw HD-EMG, i.e. joint distribution of instantaneous EMG amplitude over the electrode array, could also be a useful feature in identification of motion intention. Furthermore, in the literature, features are often calculated for each channel separately and then selected prior the classification using the, e.g., sequential method (Hargrove et al., 2009; Li et al., 2017), selection based on common spatial patterns (Geng et al., 2014), or based on the independent component analysis clustering (Naik et al., 2016). Modes of the HD-EMG density function could be correlated with the channels with discriminative information and could be a useful tool in channel selection.

Finally, the mean shift algorithm can be used for clustering and, since it was shown that the algorithm is most effective in low-dimensional data, image segmentation is one of its most successful applications (Comaniciu and Meer, 2002). A mode of the density estimate, or in this case, a channel selected by the mean shift algorithm, can be considered as a cluster representative (Hennig et al., 2015), related to the possible image segments, where spatial (pixel locations) and range features (the intensity of the grayscale value) are considered. The advantage of the mean shift is that it can be used for clustering non-convex shapes, albeit, it could segment complex non-convex regions in the activation maps. Since segmentation of the muscle activation map can improve the neuromuscular activity estimation (Vieira et al., 2010), this could be a reason why mean shift features improved the performance of the movement detection system compared with previously published attributes. In addition, the algorithm only requires setting one parameter, bandwidth (h) and, unlike in the similar methods, it is not necessary to define the number of expected clusters. This is a big advantage because it does not require a priori knowledge on the number of clusters.

As a limitation of the study, it should be noted that the proposed features were tested only in highly controlled conditions of isometric contractions. The experiments during non-isometric contractions should be performed in order to validate the quality of the features in dynamic and more natural movements. Also, the experiment included only four tasks related to the elbow joint. Further analysis should include higher number of more complex tasks related to hand and shoulder. Moreover, all results were obtained during offline analysis. To evaluate practical aspects of the features, the experiment should be repeated using online identification and considering multiple transitions between tasks.

3.3 Main contributions

The original contributions provided by the compendium of publications of this thesis are:

- The definition of a novel pattern-recognition algorithm for task and force identification. The method was based on combination of intensity and spatial distribution of intensity of myoelectric signal. The algorithm was validated in the group of patients with incomplete spinal cord injury in terms of robustness during slow time dependent changes, such as fatigue and drying of conductive gel. The results prove the existence of repeatable co-activation pattern in intensity and spatial distribution for each patient. Furthermore, the pattern exist for different tasks, but also for different effort levels

- The co-activation pattern in intensity and its spatial distribution of HD-EMG was identified for the group of patients with spinal cord injury. After the injury there is a coherence between activation patterns of different patients, both task-related and force-related. This coherence can be observed in intensity of HD-EMG, but also in spatial distribution of intensity. Furthermore, greater similarity was found within the group of patients with similar level of injury. This result implies the possibility of building assistive/rehabilitation device for the group of patients with significantly lower training time.

- Definition of novel statistical spatial feature derived from the HD-EMG. It was used for identification of task and effort level in group of healthy subjects. This feature is based on the probability density function of the HD-EMG activation map.

3.4 Future Work

The work developed in this thesis open new possibilities in the brain research line of the *BIOsignal Analysis for Rehabilitation and Therapy Research Group (BIOART)* to which the candidate belongs. Some of the most interesting further possibilities are the following:

Dynamic contractions

The use of spatial information of myoelectric activity is a novel method which already showed very good results in identification of tasks, both in healthy subjects and in patients with incomplete spinal cord injury during isometric contractions. Isometric contractions are standard to the field of work, that is, pattern recognition for control of human-machine interfaces and are a good starting point to test the new feature with respect to more classical features. Recordings during isometric contractions provide measurements with more controlled conditions, i.e., minimized influences related to relative shift of recording electrodes with respect to source of the signal – muscle fiber. Therefore it is a good practice to start using new features in graduate analysis in order to establish reliable and precisely the circumstances in which features are useful. However, further studies are necessary to consider non-isometric contractions, which are closer to real conditions. One of this study was already performed within the scope of the thesis and the results are published:

Rojas-Martínez, M., Alonso, J.F., Jordanić, M., Romero, S., Mañanas, M.A. **Identificación de tareas isométricas y dinámicas del miembro superior basada en EMG de alta densidad**. *Revista Iberoamericana de Automática e Informática Industrial*, Accepted for publication 2017, JCR 0.390, Q4 in Automation and Control Systems (57/60)

Generalized mean shift approach

In chapter 5 is explained the motor task identification algorithm that uses the novel spatial feature. This spatial feature is based on the modes of the probability density function of HD-EMG activation maps. Instead, the viability of features based on the modes of the probability density function of raw HD-EMG signal should be explored. Since the information is partially lost by calculating the RMS value of the signal to obtain the activation maps, using joint distribution of instantaneous EMG amplitude over the electrode could provide higher identification results.

Mean shift approach for channel selection

Geng et al. recently proposed a more advanced channel selection method based on common spatial patterns (Geng et al., 2014) and Naik et al. propose the channel selection based on the independent component analysis (Naik et al., 2016). Modes of the HD-EMG density function, a novel feature proposed in chapter 5 could be correlated with the channels with discriminative information and could be a useful tool in channel selection.

Real time application

The task identification system cannot find application without ability of online processing. Therefore, appropriate recording device along with an optimized processing unit should be built. The device should be able to process the task identification in real time using optimized firmware.

Hybrid brain-computer interface

The fusion of EEG and EMG could further improve the results of upper-limb task identification, the study we performed using only HD-EMG recordings both in healthy subjects and iSCI patients. This type of study can have impact on numerous fields of application including brain – computer interfaces (BCI). A goal could be to exploit the fusion of cerebral and neuromuscular information and to quantify the improvements when the innovative technique of HD-EMG is joined with the cerebral activity, what was recently called by the research community a *hybrid BCI* (Muller-Putz et al., 2015; Rohm et al., 2013).

Increase of identification fidelity

Fidelity of the identification could be increased further by using an adaptive model of classifier that is being constantly updated throughout the exercise in order to compensate for the changes in the myoelectric signal caused by, e.g., fatigue. There are several recent publications on this subject (Hahne et al., 2015; Vidovic et al., 2016; Sensinger et al., 2009).

Spatial distribution of frequency

Features extracted from frequency/scale domain proved to be very useful in identification of motor task (Oskoei and Hu, 2007). In future works, it would be interesting to investigate the spatial distribution of frequency over the muscle in search of the discriminative feature.

3.5 Publications derived from the thesis

3.5.1 Journal papers

- Jordanić, M., Rojas-Martínez, M., Mañanas, M.A., Alonso, J.F., Marateb, H.R. A Novel Spatial Feature for the Identification of Motor Tasks Using High-Density Electromyography. *Sensors*, 17(7): 1597, 2017, JCR 2.077, Q1 in Instruments and instrumentation (10/58)

- Rojas-Martínez, M., Alonso, J.F., Jordanić, M., Romero, S., Mañanas, M.A. Identificación de tareas isométricas y dinámicas del miembro superior basada en EMG de alta densidad. *Revista Iberoamericana de Automática e Informática Industrial*, Accepted for publication 2017, JCR 0.390, Q4 in Automation and Control Systems (57/60)

- Jordanić, M., Rojas-Martínez, M., Mañanas, M.A., Alonso, J.F. Prediction of isometric motor tasks and effort levels based on high-density EMG in patients with incomplete spinal cord injury. *Journal of Neural Engineering*, 13(4): 46002, 2016, JCR 3.465, Q1 in Biomedical Engineering (13/77)

- Jordanić, M., Rojas-Martínez, M., Mañanas, M.A., Alonso, J.F. Spatial distribution of HD-EMG improves identification of task and force in patients with incomplete spinal cord injury. *Journal of NeuroEngineering and Rehabilitation*, 13(1): 41, 2016, JCR 3.222, Q1 in Rehabilitation (3/65)

3.5.2 Conference papers

- Jordanić, M., Rojas-Martínez, M., Mañanas, M.A. Muscle pattern from HD-EMG applied to identification of movement intention. Summer School on Neurorehabilitation (SSNR 2015), 2015, Valencia, Spain

- Jordanić, M., Rojas-Martínez, M., Mañanas, M.A., Alonso, J.F. Use of frequency features of HD-EMG in identification of upper-limb motor task. *Cognitive Area Networks*, 4(1): 19:23, 9. Simposio CEA de Bioingeniería: Interfaces Cerebro-Máquina y Neurotecnologías para la Asistencia y la Rehabilitación, 2017, Badalona, Spain

- Jordanić, M., Rojas-Martínez, M., Alonso, J.F., Migliorelli, C. Mañanas, M.A. Identificación de Contracciones Isométricas de la Extremidad Superior en Pacientes con Lesión Medular Incompleta mediante Características Espectrales de la Electromiografía de Alta Densidad (HD-EMG). Jornadas de Automática (Bioinenienería), 2017, Gijon, Spain

Bibliography

Baker, J. J., Scheme, E., Englehart, K., Hutchinson, D. T., and Greger, B. Continuous detection and decoding of dexterous finger flexions with implantable myoelectric sensors. *IEEE Transactions on Neural Systems and Rehabilitation Engineering*, 18(4):424–432, 2010.

Beck, T. W., DeFreitas, J. M., and Stock, M. S. Accuracy of three different techniques for automatically estimating innervation zone location. *Computer Methods and Programs in Biomedicine*, 105(1):13–21, 2012.

Boyd, S. and Vandenberghe, L. *Convex optimization.* Cambridge University Press, 2004.

Chu, J. U., Moon, I., and Mun, M. S. A Real-Time EMG Pattern Recognition System Based on Linear-Nonlinear Feature Projection for a. *IEEE Transactions on Biomedical Engineering*, 53(11):2232–2239, 2006.

Cifrek, M., Tonković, S., and Medved, V. Measurement and analysis of surface myoelectric signals during fatigued cyclic dynamic contractions. *Measurement: Journal of the International Measurement Confederation*, 27(2):85–92, 2000.

Clancy, E., Morin, E. L., and Merletti, R. Sampling, noise-reduction and amplitude estimation issues in surface electromyography. *Journal of Electromyography and Kinesiology*, 12(1):1–16, 2002.

Comaniciu, D. and Meer, P. Mean shift: a robust approach toward feature space analysis. *IEEE Transactions on Pattern Analysis and Machine Intelligence*, 24(5):603–619, 2002.

De Luca, C. J. Physiology and Mathematics of Myoelectric Signals. *IEEE Transactions on Biomedical Engineering*, 26(6):313–325, 1979.

De Luca, C. J. Myoelectrical manifestations of localized muscular fatigue in humans. *Critical Reviews in Biomedical Engineering*, 11(4):251–79, jan 1984.

Dipietro, L., Ferraro, M., Palazzolo, J. J., Krebs, H. I., Volpe, B. T., and Hogan, N. Customized interactive robotic treatment for stroke: EMG-triggered therapy. *IEEE Transactions on Neural Systems and Rehabilitation Engineering*, 13(3):325–334, 2005.

Duchateau, J. and Enoka, R. M. Human motor unit recordings: Origins and insight into the integrated motor system. *Brain Research*, 1409:42–61, 2011.

Englehart, K. and Hudgins, B. A robust, real-time control scheme for multifunction myoelectric control. *IEEE Transactions on Biomedical Engineering*, 50(7):848–854, 2003.

Englehart, K., Hudgins, B., Parker, P. a., and Stevenson, M. Classification of the myoelectric signal using time-frequency based representations. *Medical Engineering and Physics*, 21(6-7):431–438, 1999.

Englehart, K., Hudgins, B., and Parker, P. A. A wavelet-based continuous classification scheme for multifunction myoelectric control. *IEEE Transactions on Biomedical Engineering*, 48(3): 302–11, 2001.

Englehart, K., Hudgins, B., and Chan, A. D. C. Continuous multifunction myoelectric control using pattern recognition. *Technology and Disability*, 15(2):95–103, 2003.

Farina, D., Févotte, C., Doncarli, C., and Merletti, R. Blind separation of linear instantaneous mixtures of nonstationary surface myoelectric signals. *IEEE Transactions on Biomedical Engineering*, 51(9):1555–67, 2004.

Farina, D., Holobar, A., Merletti, R., and Enoka, R. M. Decoding the neural drive to muscles from the surface electromyogram. *Clinical Neurophysiology*, 121(10):1616–1623, 2010.

Farina, D., Jiang, N., Rehbaum, H., Holobar, A., Graimann, B., Dietl, H., and Aszmann, O. C. The extraction of neural information from the surface EMG for the control of upper-limb prostheses: emerging avenues and challenges. *IEEE Transactions on Neural Systems and Rehabilitation Engineering*, 22(4):797–809, 2014a.

Farina, D., Merletti, R., and Enoka, R. M. The extraction of neural strategies from the surface EMG: an update. *Journal of applied physiology*, 117(11):1215–30, 2014b.

Farrell, T. R. and Weir, R. F. F. A comparison of the effects of electrode implantation and targeting on pattern classification accuracy for prosthesis control. *IEEE Transactions on Biomedical Engineering*, 55(9):2198–211, 2008.

Fougner, A., Scheme, E., Chan, A. D. C., Englehart, K., and Stavdahl, Ø. Resolving the Limb Position Effect in Myoelectric Pattern Recognition. *IEEE Transactions on Neural Systems and Rehabilitation Engineering*, 19(6):644–651, 2011.

Fougner, A., Stavdahl, O., Kyberd, P. J., Losier, Y. G., and Parker, P. a. Control of upper limb prostheses: Terminology and proportional myoelectric control - A review. *IEEE Transactions on Neural Systems and Rehabilitation Engineering*, 20(5):663–677, 2012.

Freund, H. J., Büdingen, H. J., and Dietz, V. Activity of Single Motor Units from Human Forearm Muscles during Voluntary Isometric Contractions. *Journal of Neurophysiology*, 38 (4):933–46, jul 1975.

Geng, Y., Zhang, X., Zhang, Y.-T., and Li, G. A novel channel selection method for multiple motion classification using high-density electromyography. *Biomedical Engineering Online*, 13:102, 2014.

Georgakis, A., Stergioulas, L., and Giakas, G. Fatigue analysis of the surface EMG signal in isometric constant force contractions using the averaged instantaneous frequency. *IEEE Transactions on Biomedical Engineering*, 50(2):262–265, 2003.

Ghaderi, P. and Marateb, H. R. Muscle Activity Map Reconstruction from High Density Surface EMG Signals With Missing Channels Using Image Inpainting and Surface Reconstruction Methods. *IEEE Transactions on Biomedical Engineering*, 64(7):1513–1523, 2017.

Grouven, U., Bergel, F., and Schultz, A. Implementation of linear and quadratic discriminant analysis incorporating costs of misclassification. *Computer Methods and Programs in Biomedicine*, 49(1):55–60, jan 1996.

Hägg, G. Electromyographic fatigue analysis based on the number of zero crossings. *Pflügers Archiv - European Journal of Physiology*, 391(1):78–80, 1981.

Hahne, J. M., Dähne, S., Hwang, H. J., Müller, K. R., and Parra, L. C. Concurrent Adaptation of Human and Machine Improves Simultaneous and Proportional Myoelectric Control. *IEEE Transactions on Neural Systems and Rehabilitation Engineering*, 23(4):618–627, 2015.

Hakonen, M., Piitulainen, H., and Visala, A. Current state of digital signal processing in myoelectric interfaces and related applications. *Biomedical Signal Processing and Control*, 18: 334–359, 2015.

Hargrove, L., Englehart, K., and Hudgins, B. A training strategy to reduce classification degradation due to electrode displacements in pattern recognition based myoelectric control. *Biomedical Signal Processing and Control*, 3(2):175–180, 2008.

Hargrove, L., Li, G., Englehart, K., and Hudgins, B. Principal Components Analysis Preprocessing for Improved Classification Accuracies in Pattern-Recognition-Based Myoelectric Control. *IEEE Transactions on Biomedical Engineering*, 56(5):1407–1414, 2009.

Hargrove, L. J., Englehart, K., and Hudgins, B. A comparison of surface and intramuscular myoelectric signal classification. *IEEE Transactions on Biomedical Engineering*, 54(5):847–853, 2007.

He, J., Zhang, D., Sheng, X., Li, S., and Zhu, X. Invariant surface EMG feature against varying contraction level for myoelectric control based on muscle coordination. *IEEE Journal of Biomedical and Health Informatics*, 19(3):874–882, 2015.

Henneberg, K. Principles of Electromyography. In Bronzino, J., editor, *The Biomedical Engineering Handbook.* CRC Press, Boca Raton, second edition, 1999.

Henneman, E., Somjen, G., and Carpenter, D. O. Functional Significance of Cell Size in Spinal Motoneurons. *Journal of Neurophysiology*, 28(3), 1965.

Hennig, C., Meila, M., Murtagh, F., and Rocci, R. *Handbook of Cluster Analysis.* CRC Press, 2015.

Hermens, H. and Freriks, B. *SENIAM 9: European Recommendations for Surface ElectroMyoGraphy, results of the SENIAM project (CD).* Roessingh Research and Development, 1999.

Hogan, N., Krebs, H. I., Rohrer, B., Palazzolo, J. J., Dipietro, L., Fasoli, S. E., Stein, J., Hughes, R., Frontera, W. R., Lynch, D., and Volpe, B. T. Motions or muscles? Some behavioral factors underlying robotic assistance of motor recovery. *Journal of Rehabilitation Research and Development*, 43(5):605–618, 2006.

Holobar, a. and Farina, D. Blind source identification from the multichannel surface electromyogram. *Physiological measurement*, 35(7):143–165, 2014.

Holobar, A. and Zazula, D. Multichannel Blind Source Separation Using Convolution Kernel Compensation. *IEEE Transactions on Signal Processing*, 55(9):4487–4496, sep 2007.

Holobar, A., Minetto, M. A., Botter, A., Negro, F., and Farina, D. Experimental Analysis of Accuracy in the Identification of Motor Unit Spike Trains From High-Density Surface EMG. *IEEE Transactions on Neural Systems and Rehabilitation Engineering*, 18(3):221–229, 2010.

Holtermann, A., Roeleveld, K., and Karlsson, J. S. Inhomogeneities in muscle activation reveal motor unit recruitment. *Journal of Electromyography and Kinesiology*, 15(2):131–137, 2005.

Hudgins, B., Parker, P., and Scott, R. N. A new strategy for multifunction myoelectric control. *IEEE Transactions on Biomedical Engineering*, 40(1):82–94, 1993.

Jiang, N., Dosen, S., Muller, K.-R., and Farina, D. Myoelectric Control of Artificial Limbs—Is There a Need to Change Focus? [In the Spotlight]. *IEEE Signal Processing Magazine*, 29(5): 152–150, 2012.

Kamavuako, E. N., Rosenvang, J. C., Horup, R., Jensen, W., Farina, D., and Englehart, K. B. Surface versus untargeted intramuscular EMG based classification of simultaneous and dynamically changing movements. *IEEE Transactions on Neural Systems and Rehabilitation Engineering*, 21(6):992–998, 2013.

Knaflitz, M. and Bonato, P. Time-frequency methods applied to muscle fatigue assessment during dynamic contractions. *Journal of Electromyography and Kinesiology*, 9(5):337–50, oct 1999.

Kupa, E. J., Roy, S. H., Kandarian, S. C., and De Luca, C. J. Effects of muscle fiber type and size on EMG median frequency and conduction velocity. *Journal of Applied Physiology*, 79 (1):23–32, 1995.

Lago, P. and Jones, N. B. Effect of motor-unit firing time statistics on E.M.G. spectra. *Medical & biological engineering & computing*, 15(6):648–55, 1977.

Li, G., Schultz, A. E., and Kuiken, T. A. Quantifying pattern recognition- based myoelectric control of multifunctional transradial prostheses. *IEEE Transactions on Neural Systems and Rehabilitation Engineering*, 18(2):185–192, 2010.

Li, X., Samuel, O. W., Zhang, X., Wang, H., Fang, P., and Li, G. A motion-classification strategy based on sEMG-EEG signal combination for upper-limb amputees. *Journal of NeuroEngineering and Rehabilitation*, 14(1):2, 2017.

Li, Y., Chen, X., Zhang, X., and Zhou, P. Several practical issues toward implementing myoelectric pattern recognition for stroke rehabilitation. *Medical Engineering and Physics*, 36(6): 754–760, 2014.

Liddell, E. G. T. and Sherrington, C. S. Recruitment and some other Features of Reflex Inhibition. *Proceedings of the Royal Society of London B: Biological Sciences*, 97(686):488–518, 1925.

Lindstrom, L. and Magnusson, R. Interpretation of myoelectric power spectra: A model and its applications. *Proceedings of the IEEE*, 65(5):653–662, 1977.

Liu, J. and Zhou, P. A novel myoelectric pattern recognition strategy for hand function restoration after incomplete cervical spinal cord injury. *IEEE Transactions on Neural Systems and Rehabilitation Engineering*, 21(1):96–103, 2013.

Liu, S., Guo, J., Meng, J., Wang, Z., Yao, Y., Yang, J., Qi, H., and Ming, D. Abnormal EEG Complexity and Functional Connectivity of Brain in Patients with Acute Thalamic Ischemic Stroke. *Computational and Mathematical Methods in Medicine*, 2016:1–9, 2016.

Madeleine, P., Leclerc, F., Arendt-Nielsen, L., Ravier, P., and Farina, D. Experimental muscle pain changes the spatial distribution of upper trapezius muscle activity during sustained contraction. *Clinical Neurophysiology*, 117(11):2436–45, 2006.

Marateb, H. R., McGill, K. C., and Webster, J. G. Electromyographic (Emg) Decomposition. In *Wiley Encyclopedia of Electrical and Electronics Engineering*. John Wiley & Sons, Inc, 1999.

Marateb, H. R., Farahi, M., Rojas, M., Mañanas, M. A., Farina, D., and Rix, H. Detection of Multiple Innervation Zones from Multi-Channel Surface EMG Recordings with Low Signal-to-Noise Ratio Using Graph-Cut Segmentation. *PLOS ONE*, 11(12), 2016.

Marchal-Crespo, L. and Reinkensmeyer, D. J. Review of control strategies for robotic movement training after neurologic injury. *Journal of Neuroengineering and Rehabilitation*, 6:20, 2009.

McLachlan, G. J. *Discriminant analysis and statistical pattern recognition.* John Wiley and Sons, New York, USA, 2004.

Merletti, R. and Farina, D. *Surface Electromyography: Physiology, Engineering, and Applications.* Wiley-IEEE Press, Hoboken, New Jersey (USA), 2016.

Merletti, R. and Lo Conte, L. R. Surface EMG signal processing during isometric contractions. *Journal of Electromyography and Kinesiology*, 7(4):241–250, 1997.

Merletti, R. and Parker, P. *Electromyography : physiology, engineering, and noninvasive applications.* Wiley-IEEE Press, 2004.

Merletti, R., Aventaggiato, M., Botter, A., Holobar, A., Marateb, H., and Vieira, T. M. M. Advances in surface EMG: recent progress in detection and processing techniques. *Critical Reviews in Biomedical Engineering*, 38(4):305–45, 2010.

Muller-Putz, G., Leeb, R., Tangermann, M., Hohne, J. H., Kubler, A. K., Cincotti, F., Mattia, D., Rupp, R., Muller, K. R., and Millan, J. D. R. Towards Noninvasive Hybrid Brain–Computer Interfaces: Framework, Practice, Clinical Application, and Beyond. *Proceedings of the IEEE*, 103(6):926 – 943, 2015.

Naik, G. R., Kumar, D. K., and Weghorn, H. Performance comparison of ICA algorithms for Isometric Hand gesture identification using Surface EMG. In *3rd International Conference on Intelligent Sensors, Sensor Networks and Information*, pages 613–618. IEEE, 2007.

Naik, G. R., Al-Timemy, A. H., and Nguyen, H. T. Transradial Amputee Gesture Classification Using an Optimal Number of sEMG Sensors: An Approach Using ICA Clustering. *IEEE Transactions on Neural Systems and Rehabilitation Engineering*, 24(8):837–846, 2016.

Nazmi, N., Abdul Rahman, M., Yamamoto, S.-I., Ahmad, S., Zamzuri, H., and Mazlan, S. A Review of Classification Techniques of EMG Signals during Isotonic and Isometric Contractions. *Sensors*, 16(8):1304, 2016.

OpenStax. Skeletal Muscle. OpenStax CNX, http://cnx.org/contents/6df8aab3-1741-4016-b5a9-ac51b52fade0@3., 2013.

Oskoei, M. A. and Hu, H. Myoelectric control systems-A survey. *Biomedical Signal Processing and Control*, 2(4):275–294, 2007.

Park, S. H. and Lee, S. P. EMG pattern recognition based on artificial intelligence techniques. *IEEE Transactions on Rehabilitation Engineering*, 6(4):400–405, 1998.

Parker, P. A. and Scott, R. N. Myoelectric control of prostheses. *Critical reviews in biomedical engineering*, 13(4):283–310, 1986.

Phinyomark, A., Limsakul, C., and Phukpattaranont, P. A Novel Feature Extraction for Robust EMG Pattern Recognition. *Journal of Computing*, 1(1):71–80, 2009.

Phinyomark, A., Phukpattaranont, P., and Limsakul, C. Feature reduction and selection for EMG signal classification. *Expert Systems with Applications*, 39(8):7420–7431, 2012a.

Phinyomark, A., Thongpanja, S., Hu, H., Phukpattaranont, P., and Limsakul, C. *Computational Intelligence in Electromyography Analysis - A Perspective on Current Applications and Future Challenges*. InTech, 2012b.

Rohm, M., Schneiders, M., Müller, C., Kreilinger, A., Kaiser, V., Müller-Putz, G. R., and Rupp, R. Hybrid brain-computer interfaces and hybrid neuroprostheses for restoration of upper limb functions in individuals with high-level spinal cord injury. *Artificial Intelligence in Medicine*, 59(2):133–142, 2013.

Rojas-Martínez, M. *Analysis of Forearm Muscles Activity by Means of New Protocols of Multichannel EMG Signals Recording and Processing*. Phd dissertation, Polytechnic University of Catalonia, 2012.

Rojas-Martínez, M., Mañanas, M. a., and Alonso, J. F. High-density surface EMG maps from upper-arm and forearm muscles. *Journal of Neuroengineering and Rehabilitation*, 9:85, jan 2012.

Rojas-Martínez, M., Mañanas, M. a., Alonso, J. F., and Merletti, R. Identification of isometric contractions based on High Density EMG maps. *Journal of Electromyography and Kinesiology*, 23(1):33–42, 2013.

Sensinger, J., Lock, B., and Kuiken, T. Adaptive Pattern Recognition of Myoelectric Signals: Exploration of Conceptual Framework and Practical Algorithms. *IEEE Transactions on Neural Systems and Rehabilitation Engineering*, 17(3):270–278, 2009.

Sherrington, C. S. Remarks on some Aspects of Reflex Inhibition. *Proceedings of the Royal Society of London B: Biological Sciences*, 97(686):519–545, 1925.

Simon, A. M., Hargrove, L. J., Lock, B. a., and Kuiken, T. a. A decision-based velocity ramp for minimizing the effect of misclassifications during real-time pattern recognition control. *IEEE Transactions on Biomedical Engineering*, 58(8):2360–2368, 2011.

Soares, F. A., Carvalho, J. L. A., Miosso, C. J., de Andrade, M. M., and da Rocha, A. F. Motor unit action potential conduction velocity estimated from surface electromyographic signals using image processing techniques. *BioMedical Engineering Online*, 14(1):84, 2015.

Squire, J. *Muscle: design, diversity, and disease*. Benjamin/Cummnigs, Menlo Park, CA, USA, 1986.

Srhoj-Egekher, V., Cifrek, M., and Medved, V. The application of Hilbert-Huang transform in the analysis of muscle fatigue during cyclic dynamic contractions. *Medical & biological engineering & computing*, 49(6):659–69, jun 2011.

Stango, A., Negro, F., and Farina, D. Spatial Correlation of High Density EMG Signals Provides Features Robust to Electrode Number and Shift in Pattern Recognition for Myocontrol. *IEEE Transactions on Neural Systems and Rehabilitation Engineering*, 23(2):189–198, 2015.

Staudenmann, D., Roeleveld, K., Stegeman, D. F., and van Dieen, J. H. Methodological aspects of SEMG recordings for force estimation - A tutorial and review. *Journal of Electromyography and Kinesiology*, 20(3):375–387, 2010.

Staudenmann, D., van Dieën, J. H., Stegeman, D. F., and Enoka, R. M. Increase in heterogeneity of biceps brachii activation during isometric submaximal fatiguing contractions: a multichannel surface EMG study. *Journal of neurophysiology*, 111(5):984–90, 2014.

Stulen, F. B. and De Luca, C. J. Frequency Parameters of the Myoelectric Signal as a Measure of Muscle Conduction Velocity. *IEEE Transactions on Biomedical Engineering*, 28(7):515–523, 1981.

Tkach, D., Huang, H., and Kuiken, T. a. Study of stability of time-domain features for electromyographic pattern recognition. *Journal of Neuroengineering and Rehabilitation*, 7:21, 2010.

Tucker, K., Falla, D., Graven-Nielsen, T., and Farina, D. Electromyographic mapping of the erector spinae muscle with varying load and during sustained contraction. *Journal of Electromyography and Kinesiology*, 19(3):373–9, 2009.

Vaca Benitez, L. M., Tabie, M., Will, N., Schmidt, S., Jordan, M., and Kirchner, E. A. Exoskeleton technology in rehabilitation: Towards an EMG-based orthosis system for upper limb neuromotor rehabilitation. *Journal of Robotics*, 2013:13, 2013.

Vidovic, M. M.-C., Hwang, H.-J., Amsuss, S., Hahne, J. M., Farina, D., and Muller, K.-R. Improving the Robustness of Myoelectric Pattern Recognition for Upper Limb Prostheses by Covariate Shift Adaptation. *IEEE Transactions on Neural Systems and Rehabilitation Engineering*, 24(9):961–970, 2016.

Vieira, T. M. M., Merletti, R., and Mesin, L. Automatic segmentation of surface EMG images: Improving the estimation of neuromuscular activity. *Journal of Biomechanics*, 43(11):2149–58, 2010.

Widmaier, E. P., Raff, H., and Strang, K. T. *Vander's Human Physiology: The mechanisms of Body Function*. McGraw-Hill Higher Education, 9th editio edition, 2003.

Young, A. J., Hargrove, L. J., and Kuiken, T. A. The Effects of Electrode Size and Orientation on the Sensitivity of Myoelectric Pattern Recognition Systems to Electrode Shift. *IEEE Transactions on Biomedical Engineering*, 58(9):2537–2544, 2011.

Young, A. J., Smith, L. H., Rouse, E. J., and Hargrove, L. J. Classification of simultaneous movements using surface EMG pattern recognition. *IEEE Transactions on Biomedical Engineering*, 60(5):1250–1258, 2013.

Zardoshti-Kermani, M., Wheeler, B., Badie, K., and Hashemi, R. EMG feature evaluation for movement control of upper extremity prostheses. *IEEE Transactions on Rehabilitation Engineering*, 3(4):324–333, 1995.

Zhang, X. and Zhou, P. High-Density Myoelectric Pattern Recognition Toward Improved Stroke Rehabilitation. *IEEE Transactions on Biomedical Engineering*, 59(6):1649–1657, 2012.

Zwarts, M. J. and Stegeman, D. F. Multichannel surface EMG: basic aspects and clinical utility. *Muscle & nerve*, 28(1):1–17, 2003.

Zwarts, M. J., Lapatki, B. G., Kleine, B. U., and Stegeman, D. F. Surface EMG: how far can you go? *Supplements to Clinical Neurophysiology*, 57:111–9, 2004.

Appendix A

Pattern recognition

Pattern recognition is a classification technique and the principle by which it is performed is learned independently from the data, i.e., training set. There are two main types of pattern recognition: supervised and unsupervised. Supervised pattern recognition implies that the classes of the training set are known and are used to obtain the model. New inputs are identified as one of the predetermined classes. On the other hand, unsupervised pattern recognition is used when no labels are available and samples are assigned to unknown classes. This technique is more appropriate for the clustering problem because the classes are determined automatically by the system, whereas supervised approach is more appropriate for the classification because classes are defined by the system designer, and, therefore, it is usually used in task identification based on EMG.

In statistical pattern recognition, each sample is composed of m measures that form the pattern, i.e., features $(x_0, x_1, \ldots, x_{m-1})$. The objective of the algorithm is to obtain a decision rule, i.e., the decision boundary which separates well samples of different classes. There are many *state-of-the-art* classifiers that use various principles to construct these boundaries. However, many researchers agree that the fidelity of the classification in EMG applications depends mostly on selection of features (Hakonen et al., 2015). In other words, with appropriate selection of features, all classifiers will give similar classification result. A short introduction is provided on the two methods used in the thesis: Linear Discriminant Analysis and Support Vector Machine. Although the SVM is superior in classification performance, the LDA is commonly used in myocontrol applications because of its simplicity and performance in real-time. However, with the increasing computational power of new computer generations, SVM could become more common in these applications.

A.1 Linear Discriminant Analysis

All models are wrong; some models are useful.
George E. P. Box

Linear Discriminant Analysis is a computationally simple and efficient classifier with linear decision boundary and it is based on the Bayesian equation (McLachlan, 2004). In a classical problem with n samples in training set, which consist of m features, the dataset of available samples is a matrix of dimension $[n \times m]$, whereas the label that describes the belonging of each sample to one of the classes is y, where $y \in (0, 1, 2, ..., K-1)$.

According to Bayesian equation, the probability that a sample $\mathbf{x}_0$ belongs to a class k is equivalent to the:

$$P(y = k \mid \mathbf{x} = \mathbf{x}_0) = \frac{P(\mathbf{x} = \mathbf{x}_0 \mid y = k)\ P(y = k)}{P(\mathbf{x} = \mathbf{x}_0)} \tag{A.1}$$

, where k represents the class. Term $P(\mathbf{x} = \mathbf{x}_0 \mid y = k)$ is called the *class-conditional* probability and describes the probability that the sample with exact features $\mathbf{x}_0$ is encountered within the group of samples belonging to the class k. Term $P(y = k)$ is called the *a priori* probability and describes the probability that the sample belonging to the class k is found within the group of all samples, regardless of the features. Finally, the term $P(\mathbf{x} = \mathbf{x}_0)$ is called the *marginal* probability and describes the probability of finding the sample with exact set of features in the dataset, regardless of the class. Marginal probability can be written as a sum of class-conditional probabilities multiplied by the a priori probabilities for each class:

$$\begin{aligned} P(\mathbf{x} = \mathbf{x}_0) = P(\mathbf{x} = \mathbf{x}_0 \mid y = 1)\ P(y = 1) + \\ P(\mathbf{x} = \mathbf{x}_0 \mid y = 2)\ P(y = 2) + \cdots + \\ P(\mathbf{x} = \mathbf{x}_0 \mid y = K)\ P(y = K) \end{aligned} \tag{A.2}$$

Following the Bayesian theory, the hypothesis, i.e., the predicted class of a sample $\mathbf{x}_0$ is chosen as the class which has the highest probability $P(y = k \mid \mathbf{x} = \mathbf{x}_0)$:

$$h(\mathbf{x}_0) = \underset{k}{\operatorname{argmax}}\, P(y = k \mid \mathbf{x} = \mathbf{x}_0) \tag{A.3}$$

Statistically speaking, this is the best possible classifier. The problem arises in the implementation. The exact probability density functions are unknown and have to be estimated from the available data, which is the source of error. Estimated version of the stated probabilities will be marked with a different symbols to stress out the fact they are just an estimates:

$$p_k(\mathbf{x}) \coloneqq P(y = k \mid \mathbf{x}) \tag{A.4}$$

$$g_k(\mathbf{x}) \coloneqq P(\mathbf{x} \mid y = k) \tag{A.5}$$

$$\pi_k \coloneqq P(y = k) \tag{A.6}$$

Linear Discriminant Analysis estimates marginal probability term (π_k) as a ratio of number of samples belonging to class k and the total number of samples, whereas the class-conditional probability term in the Bayesian equation is estimated as a multivariate Gaussian function:

$$g_k(\mathbf{x}) = \frac{1}{(2\pi)^{m/2}\, |\Sigma_k|^{1/2}}\ e^{-1/2(\mathbf{x}-\mu_k)^T \Sigma_k^{-1} (\mathbf{x}-\mu_k)} \tag{A.7}$$

, where m is the dimensionality of the feature space, i.e., number of features representing each sample. Function g_k is estimated class-conditional probability of class k, and μ_k and Σ_k are the mean and co-variance matrix for class k, respectively, and they are estimated from the available data as:

$$\mu_k = \frac{1}{n_k} \sum_i \mathbf{x}_i \Bigg|_{\forall \mathbf{x} \in k} \tag{A.8}$$

$$\Sigma_k = \frac{1}{n_k - K} \sum_i \Big(\mathbf{x}_i - \mu_k\Big)\Big(\mathbf{x}_i - \mu_k\Big)^T \Bigg|_{\forall \mathbf{x} \in k} \tag{A.9}$$

, where n_k represents the number of samples belonging to a class k. To simplify the model, LDA assumes that the co-variance matrices Σ_k are the same for all classes:

$$\Sigma_0 = \Sigma_1 = \cdots = \Sigma_{K-1} = \Sigma \tag{A.10}$$

and they are usually calculated using the weighted average:

$$\Sigma = \frac{\sum_{k=1}^{K} n_k \Sigma_k}{\sum_{k=1}^{K} n_k} \tag{A.11}$$

The consequence of this assumption is the linearity of the decision boundary. Without this assumption the same calculus would lead to quadratic discriminant analysis, which has non-linear boundary.

In a two class example ($y \in \{0, 1\}$), all samples on the decision boundary will have the same probability of belonging to class 0 or 1:

$$D.B. = \Big\{ \mathbf{x} \;\Big|\; P\big(y = 0 \,\big|\, \mathbf{x} = \mathbf{x}_0\big) = P\big(y = 1 \,\big|\, \mathbf{x} = \mathbf{x}_0\big) \Big\} \tag{A.12}$$

Following this idea, the decision boundary can be estimated by solving the equation:

$$\frac{g_0(\mathbf{x})\,\pi_0}{\cancel{\sum_{k=1}^{K} g_k\,\pi_k}} = \frac{g_1(\mathbf{x})\,\pi_1}{\cancel{\sum_{k=1}^{K} g_k\,\pi_k}} \tag{A.13}$$

$$\frac{1}{(2\pi)^{m/2}\,|\Sigma_0|^{1/2}}\; e^{-1/2(\mathbf{x}-\mu_0)^T \Sigma_0^{-1} (\mathbf{x}-\mu_0)}\;\; \pi_0 = \frac{1}{(2\pi)^{m/2}\,|\Sigma_1|^{1/2}}\; e^{-1/2(\mathbf{x}-\mu_1)^T \Sigma_1^{-1} (\mathbf{x}-\mu_1)}\;\; \pi_1 \tag{A.14}$$

If making the assumption on the equal co-variance matrices for both classes ($\Sigma_0 = \Sigma_1 = \Sigma$), and taking the logarithm, the equation takes the form:

$$-\frac{1}{2}\Big(\mathbf{x} - \mu_0\Big)^T \Sigma^{-1} \Big(\mathbf{x} - \mu_0\Big) + \log\Big(\pi_0\Big) = -\frac{1}{2}\Big(\mathbf{x} - \mu_1\Big)^T \Sigma^{-1} \Big(\mathbf{x} - \mu_1\Big) + \log\Big(\pi_1\Big) \tag{A.15}$$

, which can be written in the form of the linear function $x^T \beta + \alpha = 0$ as:

$$\mathbf{x}^T \Big(\Sigma^{-1}\mu_0 - \Sigma^{-1}\mu_1\Big) + \frac{1}{2}\Big(\mu_1^T \Sigma^{-1} \mu_1 - \mu_0^T \Sigma^{-1} \mu_0\Big) + \log\left(\frac{\pi_0}{\pi_1}\right) = 0 \tag{A.16}$$

This equation represents the decision boundary between two classes, i.e., all samples lying on this line will have equal probability of belonging to class 0 and class 1. It should be noted that the slope of the line depends only on the class means and co-variance matrix, whereas a priori probabilities (which are the result of number of samples belonging to class 0 or 1) have effect only on the y-intercept term, i.e., the offset of the function. This is an interesting point that demands caution. If groups are unbalanced, that is, number of samples of one group is higher than in the other group, y-intercept of the decision boundary will be affected and the classifier will be biased by this disproportion. If groups are unbalanced because of the incomplete or missing data, whereas in reality they are balanced, this can have a negative effect.

When considering multiclass classification problem, probability of a sample belonging to each class is firstly estimated by the equation:

$$p_k = -\frac{1}{2}\log|\Sigma| - \frac{1}{2}\Big(\mathbf{x} - \mu_k\Big)^T \Sigma^{-1}\Big(\mathbf{x} - \mu_k\Big) + \log\Big(\pi_k\Big) \tag{A.17}$$

and then the class is estimated as the one with the highest probability as:

$$h(\mathbf{x}) = \operatorname*{argmax}_k p_k(\mathbf{x}) \tag{A.18}$$

A.2 Support Vector Machine

Try to solve the problem directly and never solve a more general problem as an intermediate step.
Vladimir Vapnik

Support vector machine is nowadays known as a very powerful classifier with a lot of different applications. The big advantage over LDA is the fact that it is a *non-parametric* classifier. The model is not obtained using assumptions of the form of the class density function and estimation of it's parameters, which is inevitably erroneous. Instead, SVM forms the decision boundary using the samples (not their density estimates) by maximizing the distance between samples and the boundary. This was the idea Vladimir Vapnik, the inventor of this method stood for. It is better to try to solve the problem directly and simply, without many intermediate steps that can be complicated and inaccurate.

In pattern recognition, the decision rule (h) is usually obtained by multiplying the sample ($\mathbf{x}$) by predefined weights (Θ):

$$\Theta^T\mathbf{x} + \Theta_0 \tag{A.19}$$

, where Θ_0 is a constant. If samples $\mathbf{x}_0$ and $\mathbf{x}_1$ lay on the decision boundary, following statements are true:

$$\Theta^T\mathbf{x}_0 + \Theta_0 = \Theta^T\mathbf{x}_1 + \Theta_0 \tag{A.20}$$

$$\Theta^T(\mathbf{x}_0 - \mathbf{x}_1) = 0 \tag{A.21}$$

This result implies that Θ is perpendicular to the boundary:

$$\Theta \perp (\mathbf{x}_0 - \mathbf{x}_1) \tag{A.22}$$

The goal of the SVM is to find the decision boundary between two classes so that the distance between the samples and the decision boundary, i.e., the margin is maximized. The distance (d) from a sample to the decision boundary can be defined as the distance between the sample

$\mathbf{x}$ and any point lying on the boundary, $\mathbf{x}_0$, projected onto the vector Θ.

$$d = \frac{\Theta^T \left(\mathbf{x} - \mathbf{x}_0\right)}{|\Theta|} \tag{A.23}$$

Term $|\Theta|$ is introduced to normalize the vector Θ. Without the normalization the distance would depend on the norm of Θ.

Since $\mathbf{x}_0$ is on the decision boundary, the expression $\Theta^T\mathbf{x}_0 + \Theta_0 = 0$ is valid, and, therefore, the expression for the distance can be written as:

$$d = \frac{\Theta^T \mathbf{x} + \Theta_0}{|\Theta|} \tag{A.24}$$

Margin (M) can be defined as the distance from the boundary to the closest sample:

$$M = \min_i d_i \tag{A.25}$$

Depending on which side of the boundary the sample is located, the distance can be positive or negative. In order to keep it strictly positive, term y is introduced, where $y \in \{-1, 1\}$:

$$M = \min_i \left\{y_i d_i\right\} \tag{A.26}$$

$$M = \min_i \left\{ \frac{y_i \left(\Theta^T \mathbf{x}_i + \Theta_0\right)}{|\Theta|} \right\} \tag{A.27}$$

The objective is to maximize the margin M. Since Θ can be rescaled, a certain Θ exists so that $y_i \left(\Theta^T \mathbf{x}_i + \Theta_0\right) = 1$, which implies

$$\exists\Theta,\ y_i \left(\Theta^T \mathbf{x}_i + \Theta_0\right) = 1 \quad \Rightarrow \quad M = \min_i \left\{ \frac{1}{|\Theta|} \right\} \tag{A.28}$$

Therefore, to maximize the margin, a separating hyperplane should be found such that a norm of vector orthogonal to the hyperplane (Θ) is minimal.

For every point not on the boundary the following term is valid:

$$y_i \left(\Theta^T \mathbf{x}_i + \Theta_0\right) > 0 \tag{A.29}$$

Value C can be selected such that:

$$y_i \left(\Theta^T \mathbf{x}_i + \Theta_0\right) > C \tag{A.30}$$

$$y_i \left(\frac{\Theta^T \mathbf{x}_i}{C} + \frac{\Theta_0}{C} \right) > 1 \tag{A.31}$$

Since Θ and Θ_0 can be rescaled, it can be written:

$$\Theta := \frac{\Theta}{C}, \quad \Theta_0 := \frac{\Theta_0}{C} \tag{A.32}$$

, and, therefore:

$$y_i \left(\Theta^T \mathbf{x}_i + \Theta_0\right) > 1 \tag{A.33}$$

Finally the optimization problem states:

$$\min \frac{1}{2}|\Theta|^2, \quad s.t.\ y_i \left(\Theta^T \mathbf{x}_i + \Theta_0\right) > 1. \tag{A.34}$$

L_2 norm is preferred because it has continuous derivative, whereas constant $1/2$ is introduced for the mathematical convenience. The optimization is solved using Lagrangian method as:

$$L(\Theta, \Theta_0, \alpha_i) = \frac{1}{2}|\Theta|^2 - \sum_{i=1}^{n} \alpha_i \left[y_i \left(\Theta^T \mathbf{x}_i + \Theta_0\right) - 1\right] \tag{A.35}$$

$$\frac{\partial L}{\partial \Theta} = \Theta - \sum_{i=1}^{n} \alpha_i y_i \mathbf{x}_i = 0 \quad \Rightarrow \quad \Theta = \sum_{i=1}^{n} \alpha_i y_i \mathbf{x}_i \tag{A.36}$$

$$\frac{\partial L}{\partial \Theta_0} = \sum_{i=1}^{n} \alpha_i y_i = 0 \tag{A.37}$$

By rewriting the problem in A.35 in terms of dual variable α, the following expression can be obtained:

$$L(\alpha) = \sum_i \alpha_i - \frac{1}{2}\sum_j \sum_i \alpha_j \alpha_i y_j y_i \mathbf{x}_i^T \mathbf{x}_j \tag{A.38}$$

Since this function depends only on dual variable α, the solution can be obtained by maximization:

$$\max L(\alpha) \quad s.t. \quad \begin{cases} \alpha_i \geq 0 \\ \sum_i \alpha_i y_i = 0 \end{cases} \tag{A.39}$$

In this optimization problem, the objective has the form of quadratic function, whereas constraints are linear. This problem is typically solved using quadratic programming. Since it is a convex problem, the solution will always be global maximum. Once the dual variable α is found, the primal variable Θ can be calculated using the equation A.36.

In the optimization, Karush-Kuhn-Tucker conditions need to be satisfied (Boyd and Vandenberghe, 2004). One of this condition is *complementary slackness*, stating that in the optimal point (the solution of the problem), the product of dual variable and the constraint must be zero:

$$\alpha_i \left[y_i \left(\Theta^T \mathbf{x}_i + \Theta_0\right) - 1\right] = 0 \tag{A.40}$$

This condition explains well the principle of SVM. Since the dual variable must be greater or equal to zero ($\alpha \geq 0$), there are two possibilities:

1. If α is greater than zero, $\left[y_i\left(\Theta^T \mathbf{x}_i + \Theta_0\right) - 1\right]$ must equal one:

$$\alpha_i > 0 \quad \Rightarrow \quad y_i\left(\Theta^T \mathbf{x}_i + \Theta_0\right) = 1 \tag{A.41}$$

2. If $\left[y_i\left(\Theta^T \mathbf{x}_i + \Theta_0\right) - 1\right]$ is greater than zero, α must be zero:

$$y_i\left(\Theta^T \mathbf{x}_i + \Theta_0\right) > 1 \quad \Rightarrow \quad \alpha = 0 \tag{A.42}$$

Since for all samples lying on the margin, the statement

$$y_i\left(\Theta^T \mathbf{x}_i + \Theta_0\right) = 1 \tag{A.43}$$

holds, α will be greater than zero only for the samples lying on the decision hyperplane, whereas for the samples further away from the hyperplane, α will be zero. Given the fact that Θ depends on linear combination of samples weighted by α (eq. A.36), only the samples lying on the boundary will have effect in the calculation of Θ (where $\alpha > 0$), and they are called *support vectors*. The inconveniency of this approach is the fact that the data need to be linearly separable, i.e., there should not be any data on the other side of the margin, which is rarely the case in practice. For this reason it is called the *hard margin SVM*. Margin has distance one from the boundary and all points have to be distanced more or equal (constraint in eq. A.33). To relax this constrain, variable β_i is introduced for every sample $\mathbf{x}_i$, such that $\beta_i \geq 0$:s

$$y_i\left(\Theta^T \mathbf{x}_i + \Theta_0\right) \geq 1 - \beta_i \tag{A.44}$$

For points lying on the other side of the margin, β will be positive, whereas for the points on the margin or on the correct side of it, it will be zero. This is the ground assumption for *soft margin SVM*. The new optimization problem states:

$$\max \frac{1}{2}|\Theta|^2 + \gamma \sum_{i=1}^{n} \beta_i \quad s.t. \quad \begin{cases} y_i\left(\Theta^T \mathbf{x}_i + \Theta_0\right) \geq 1 - \beta_i \\ \beta_i \geq 0 \end{cases} \tag{A.45}$$

The term $\gamma \sum_{i=1}^{n} \beta_i$ is introduced to minimize this effect, whereas γ is the constant of penalization. The procedure of solving the problem is the same as in hard margin SVM, using the Lagrangian method:

$$L(\Theta, \Theta_0, \beta_i, \alpha_i, \lambda_i) = \frac{1}{2}|\Theta|^2 + \gamma \sum_{i=1}^{n} \beta_i - \sum_{i=1}^{n} \alpha_i \left[y_i\left(\Theta^T \mathbf{x}_i + \Theta_0\right) - 1 + \gamma\beta_i\right] - \sum_{i=1}^{n} \lambda_i \beta_i \tag{A.46}$$

$$\frac{\partial L}{\partial \Theta} = \Theta - \sum_{i=1}^{n} \alpha_i y_i \mathbf{x}_i = 0 \quad \Rightarrow \quad \Theta = \sum_{i=1}^{n} \alpha_i y_i \mathbf{x}_i \tag{A.47}$$

$$\frac{\partial L}{\partial \Theta_0} = \sum_{i=1}^{n} \alpha_i y_i = 0 \tag{A.48}$$

$$\frac{\partial L}{\partial \beta_i} = \gamma - \alpha_i - \lambda_i = 0 \tag{A.49}$$

By rewriting the optimization problem in terms of dual variable α, the same term can be obtained as in eq. A.38:

$$L(\alpha) = \sum_i \alpha_i - \frac{1}{2}\sum_j \sum_i \alpha_j \alpha_i y_j y_i \mathbf{x}_i^T \mathbf{x}_j \tag{A.50}$$

, and the new optimization problem states:

$$\max L(\alpha) \quad s.t. \ \begin{cases} \alpha_i \geq 0 \\ \lambda_i \geq 0 \end{cases} \tag{A.51}$$

However, since objective function $L(\alpha)$ does not depend on dual variable λ_i, the substituation can be made following the expression in eq. A.49 and the new optimization problem states:

$$\max L(\alpha) \quad s.t. \ 0 \leq \alpha_i \leq \gamma. \tag{A.52}$$

This is the only diference between hard margin SVM and soft margin SVM.

It is important to state that the optimization problem does not depend on $\mathbf{x}$, but on $\mathbf{x}^T\mathbf{x}$. This allows the use of *kernel trick* and implicitly enables nonlinear transform of the feature space at little additional cost. Usually, non-linear decision boundary can be achieved by nonlinear transform of features:

$$\mathbf{x} \to \Phi(\mathbf{x}) \tag{A.53}$$

However, this operation is computationally expensive. The solution can be achieved using kernel functions. Kernel is a function $K(x, y)$ for which:

$$K(\mathbf{x}, \mathbf{y}) = \Phi(\mathbf{x})^T \Phi(\mathbf{y}) \tag{A.54}$$

Since in the equation A.37 $\mathbf{x}$ does not appear by itself, but in a form of dot product $\mathbf{x}^T\mathbf{x}$, non-linear transform can be used in a form of kernel trick:

$$L(\alpha) = \sum_i \alpha_i - \frac{1}{2}\sum_j \sum_i \alpha_j \alpha_i y_j y_i K(\mathbf{x}_i, \mathbf{x}_j) \tag{A.55}$$

Most often used kernel is a radial basis kernel ($K_{RBF}(\mathbf{x}_i, \mathbf{x}_j)$):

$$K_{RBF}(\mathbf{x}_i, \mathbf{x}_j) = e^{\frac{-\|\mathbf{x}_i - \mathbf{x}_j\|^2}{2\sigma^2}} \tag{A.56}$$

Although SVM is conceptually designed as a two-class classifier, techniques for multiclass classification also exist, e.g. *one-versus-one* or *one-versus-all*.